Bioactive Materials 41 (2024) 672–695

Contents lists available at ScienceDirect

Bioactive Materials

journal homepage: www.keaipublishing.com/en/journals/bioactive-materials

Hormonally and chemically defined expansion conditions for organoids of biliary tree Stem Cells

Wencheng Zhang [a,b,c,1,**], Yangyang Cui [a,d,1], Mengqi Lu [a,d,1], Mingyang Xu [a,b,c,1], Yuting Li [a,b,c,1], Haimeng Song [a,b,c], Yi Luo [a,b,c], Jinjia Song [a,b,c], Yong Yang [e], Xicheng Wang [a,b,c], Lijun Liao [f], Yunfang Wang [g], Lola Reid [h,***], Zhiying He [a,b,c,*]

[a] Institute for Regenerative Medicine, Medical Innovation Center and State Key Laboratory of Cardiology, Shanghai East Hospital, School of Life Sciences and Technology, Tongji University, Shanghai, 200123, China
[b] Shanghai Engineering Research Center of Stem Cells Translational Medicine, Shanghai, 200335, China
[c] Shanghai Institute of Stem Cell Research and Clinical Translation, Shanghai, 200120, China
[d] Postgraduate Training Base of Shanghai East Hospital, Jinzhou Medical University, Jinzhou, Liaoning, 121001, China
[e] Department of General Surgery, The First Affiliated Hospital of Nanchang University, Nanchang, Jiangxi, 330006, China
[f] Department of Anesthesiology and Pain Management, Shanghai East Hospital, Tongji University School of Medicine, Shanghai, 200123, China
[g] Hepatobiliary and Pancreatic Center, Medical Research Center, Beijing Tsinghua Changgung Hospital, Beijing, 102218, China
[h] Departments of Cell Biology and Physiology, Program in Molecular Biology and Biotechnology, UNC School of Medicine, Chapel Hill, NC, 27599, United States

ARTICLE INFO

Keywords:
Biliary tree stem cells (BTSCs)
Organoids
Paracrine signals
Defined Proliferative Medium (DPM)
BTSC-Expansion-Glycogel (BEX-gel)

ABSTRACT

Wholly defined *ex vivo* expansion conditions for biliary tree stem cell (BTSC) organoids were established, consisting of a defined proliferative medium (DPM) used in combination with soft hyaluronan hydrogels. The DPM consisted of commercially available Kubota's Medium (KM), to which a set of small molecules, particular paracrine signals, and heparan sulfate (HS) were added. The small molecules used were DNA methyltransferase inhibitor (RG108), TGF- β Type I receptor inhibitor (A83-01), adenylate cyclase activator (Forskolin), and L-type Ca^{2+} channel agonist (Bay K8644). A key paracrine signal proved to be R-spondin 1 (RSPO1), a secreted protein that activates Wnts. Soluble hyaluronans, 0.05 % sodium hyaluronate, were used with DPM to expand monolayer cultures. Expansion of organoids was achieved by using DPM in combination with embedding organoids in Matrigel that was replaced with a defined thiol-hyaluronan triggered with PEGDA to form a hydrogel with a rheology [G^*] of less than 100 Pa. The combination is called the BTSC-Expansion-Glycogel-System (BEX-gel system) for expanding BTSCs as a monolayer or as organoids. The BTSC organoids were expanded more than 3000-fold *ex vivo* in the BEX-gel system within 70 days while maintaining phenotypic traits indicative of stem/progenitors. Stem-cell-patch grafting of expanded BTSC organoids was performed on the livers of $Fah^{-/-}$ mice with tyrosinemia and resulted in the rescue of the mice and restoration of their normal liver functions. The BEX-gel system for BTSC organoid expansion provides a strategy to generate sufficient numbers of organoids for the therapeutic treatments of liver diseases.

Acronyms for cell populations (or for names of antibodies derived from a specific species) are preceded by a small letter to indicate the species.

Abbreviations

m	murine
h	human
r	rabbit

Peer review under responsibility of KeAi Communications Co., Ltd.
* Corresponding author.
** Corresponding author.
*** Corresponding author.
E-mail addresses: wencheng.v.zhang@outlook.com (W. Zhang), Lola.M.Reid@gmail.com (L. Reid), zyhe@tongji.edu.cn (Z. He).
[1] Co-first authors.

https://doi.org/10.1016/j.bioactmat.2024.08.010
Received 22 March 2024; Received in revised form 25 July 2024; Accepted 13 August 2024

g goat
d donkey
ALB albumin
AFP α-fetoprotein
BEX-gel BTSC-Expansion-Glycogel
BTSCs biliary tree stem cells, hepato/pancreatic stem cells found throughout the biliary tree
CK19 keratin 19
CPS-1 Carbamoyl Phosphate Synthetase I
CS chondroitin sulfates
DPM Defined-Proliferative-Medium
EBSS Earle's Balanced Salt Solution
ECM extracellular matrix
EGF epidermal growth factor
EpCAM epithelial cell adhesion molecule
ESLDs end-stage liver diseases-induced pluripotent stem cells
ESCs human embryonic stem cells
FAH Fumarylacetoacetate Hydrolase
GAG glycosaminoglycan
GAPDH glyceraldehyde-3-phosphate dehydrogenase
HA hyaluronans
hAHeps human adult hepatocytes
hBTSCs human biliary tree stem cells
hHBs human hepatoblasts
hHpSCs human hepatic stem cells
HEPSS 4-Hydroxyerhylpiperazine-1-propanesulfonic acid Buffer Solution
HS heparan sulfate oligosaccharides
HS3ST heparan sulfate 3-O-sulfotransferase
HS-PG heparan sulfate proteoglycan
ICAM-1 intercellular cell adhesion molecule and one of the surface molecules to which HAs bind
iPSCs induced pluripotent stem cells
KLF4/KLF5 Krüppel-like factors 4 or 5, zinc finger proteins that are transcription factors in stem cells
KM Kubota's Medium, a serum-free medium designed originally for hepatoblasts but subsequently found to be generic for endodermal stem cells
KRT cytokeratin gene
LGR5 Leucine-rich repeat-containing G-protein coupled receptor 5 that binds to R-spondin
MEK mitogen-activated extracellular signal-regulated kinase
MMPs matrix metalloproteinases
NANOG a transcription factor critically involved with self-renewal
NCAM neural cell adhesion molecule
NIS sodium iodide symporter
OCT4 octamer-binding transcription factor 4, also known as **POU5F1** (POU domain, class 5, transcription factor 1), a gene expressed by stem cells
PBGs peribiliary glands in which biliary tree stem cell (BTSC) niches are found at the PBG's base that is adjacent to the peribiliary gland's interior wall
PDGs pancreatic duct glands (the glands similar to PBGs and located in the biliary tree within the pancreas)
PDX1 pancreatic and duodenal homeobox 1, a transcription factor critical for pancreatic development
PROM1 prominin 1(CD133)
SOX Sry-related HMG box
SOX2 a transcription factor that is essential for maintaining self-renewal, or pluripotency in embryonic and determined stem cells
SOX9 transcription factor associated with gene expression in liver, pancreas and intestine
SOX17 a transcription factor essential for differentiation of liver
VEGF vascular endothelial cell growth factor
WNT Wingless-type MMTV integration site family of genes for which there are multiple members
10-DPM 10-Defined-Proliferative-Medium, a wholly defined medium containing 10 factors found effective for expansion of various endodermal stem cells and used as a starting point to generate defined conditions for BTSC organoids
5-DPM 5- Defined-Proliferative-Medium, a wholly defined medium containing 5 factors found effective in eliciting expansion of BTSC organoids

1. Introduction

Human biliary tree stem cells (BTSCs) are hepato/pancreatic stem cells located in stem cell niches within intramural peribiliary glands (PBGs) throughout the intrahepatic, extrahepatic and extrapancreatic biliary tree. They yield multiple stem cell subpopulations, hepatic stem cells (HpSCs) and their descendants, hepatoblasts (HBs), in or near the canals of Hering and mediating liver regeneration, and pancreatic stem cells, in PBGs in the hepato/pancreatic common duct, and mediating pancreatic regeneration. By contrast, within the intrapancreatic biliary tree, there are only committed bipotent and unipotent progenitors, descendants of BTSCs from the hepato/pancreatic common duct, and found in niches within pancreatic duct glands (PDGs). Collectively, these BTSCs are the initiation sites to a network of maturational endodermal cell lineages mediating the formation and regeneration of liver and pancreas throughout life. Thus, BTSCs are candidates for stem cell therapies in liver and pancreatic diseases ([1–5]).

Clinical trials conducted in India have shown that transplanting a mixture of HpSCs and HBs isolated from fetal livers can rescue over 80% of patients with end-stage liver diseases (ESLDs) and provide at least 2-years of survival as compared to patients given the standard of treatment for a given disease and who died within a half year to a year. Subsequently, clinical trials in Italy found that patients transplanted with BTSCs could also be rescued [6–9]. Despite these successes, the low engraftment efficiency in livers of donor cells delivered via a vascular route and the subsequent serious problems of ectopic cell delivery of donor cells to various organs (particularly lungs and kidneys) obviated interest in pursuing full approval of these stem cell treatments beyond their use as experimental therapies in clinical trials. These limitations have been overcome by the development of stem-cell-patch grafting, novel strategies for the transplantation of organoids of stem/progenitors into liver or pancreas and resulting in nearly 100 % efficiency of engraftment and an absence of ectopic cell delivery [3,5].

This success using stem-cell-patch grafting reduced the remaining tasks for translational research for clinical programs of stem cell therapies for both liver and pancreas to a need for an expansion protocol for freshly isolated BTSCs or BTSC organoids containing BTSCs partnered with precursors to endothelia and to stellate cells. Many of the conditions for expansion have been identified in prior studies such as Kubota's Medium [10], which provides generic maintenance and expansion conditions for endodermal stem cells. Secondly, the need for organoids to be in a serum-free, hormonally defined medium for stem cells and in a hyaluronan hydrogel with very soft mechanical properties, less than 100 Pa, which is necessary for the maintenance of stem cell traits ([11,12]). Thirdly, the need to use organoids, aggregates of epithelial stem cells partnered with lineage-stage-appropriate precursors to endothelia and to stellate cells to provide the paracrine signals of epithelial-mesenchymal interactions [2,10,13–15]. Contributing to this repertoire of required factors and conditions were those identified in studies of a gastric epithelial expansion system derived from endoscopic biopsies of patients and consisting of small molecules, paracrine signals, and a matrix component.

Matrigel (Corning), an extract of the mouse Engelbreth Holm Swarm (EHS) sarcoma tumor, is enriched with basement membrane matrix components; It is commonly used for both monolayer and organoid cultures [16–20]. Major components in Matrigel are laminin (the dominant component), type IV collagen, a heparan sulfate proteoglycan

(HS-PG2; a form of perlecan), nestin, and various paracrine signals (growth factors) in complexes with the glycosaminoglycans (GAGs) present. Given the poorly defined composition of Matrigel, significant efforts have been made to replace it with defined components, particularly as needed for organoids [21–25].

We elected to test whether BTSC organoids would expand in Matrigel and, if so, to use the components in Matrigel as a guide to identify factors needed for wholly defined conditions for BTSC organoid expansion [21,24]. The other guide was by characterizing matrix components in stem cell niches or crypts of BTSCs and located at the bases of peribiliary glands (PBGs) and pancreatic duct glands (PDGs) in bile duct walls of the biliary tree. Several categories of glycosaminoglycans, hyaluronans (HA), minimally sulfated chondroitin sulfates (CS), and minimally sulfated heparan sulfates (HS), were identified as key components [26,27,28].

Here, wholly defined hydrogels that combine the components identified as the microenvironment for expansion of BTSC organoids, referred to as the BTSC-Expansion-Glycogel System, or BEX-gel System, has been established. The expanded organoids have been assessed both *ex vivo* and *in vivo* for their stem cell traits, expansion potential, and their ability to lineage restrict to mature hepatic fates. For the *in vivo* studies, the donor organoids, expanded *ex vivo* in the BEX-gel system, were transplanted using stem-cell-patch grafts onto the livers of hosts, *Fah*$^{-/-}$ mice, with a genetic condition resulting in a lethal form tyrosinemia. Stem-cell-patch grafting has proven an effective way to transplant organoids into solid organs, offering the full potential for rapid and complete engraftment with maturation of donor cells into adult fates, and yet with negligible evidence of embolism or ectopic cell delivery.

2. Results

2.1. Isolation of biliary tree stem cells from murine extra-hepatic biliary tree

BTSCs were prepared from murine extrahepatic biliary trees and that included the gallbladders, the location of late stage BTSCs. The extrahepatic biliary trees were dissected from wild type C57BL/6 mice and were dissociated using a mechanical and enzymatic digestion protocol established in prior studies [3,5]. Murine BTSCs were cultured in serum-free Kubota's medium (KM), described previously for use for BTSCs from human, porcine and murine tissues ([4,28–31]).

Purified mBTSCs and murine adult hepatocytes (mAHeps) were collected and used for RNA-sequencing. The gene expression patterns of mBTSCs and mAHeps were compared with those found previously in human subpopulations: BTSCs (hBTSCs), hepatic stem cells (hHpSCs), hepatoblasts (hHBs), and adult hepatocytes (hAHeps). The method of correlation analyses included but was not limited to Pearson, Kendall and Spearman analyses ([3–5,32]). The correlation heat map indicated that mBTSCs have genetic signatures similar to hBTSCs and hHpSCs (Fig. 1A). By contrast, mAHeps were similar to hHBs and hAHeps. Principal component analysis (PCA) proved that mBTSCs and hBTSCs are more similar in the context of all the different genes and in the context of up-regulated genes. Therefore, through PCA, we found that mBTSCs are genetically closer to hBTSCs than to hHpSCs (Fig. 1B, Figs. S1A–B).

The mBTSCs from the extrahepatic biliary tree and gallbladder form colonies on tissue culture plastic and in Kubota's Medium (KM) and can be maintained for more than three weeks. The colonies of mBTSCs were observed initially in cultures after 12 days. They underwent slow proliferation for 21 days (Fig. 1C), remaining in an undifferentiated state. Flow cytometric analyses and sorting were used to characterize the probable maturational lineage stage(s) of the cells. Previously in studies of human and porcine BTSCs ([1,28,29,33]), we found that there are multiple subpopulations, maturational lineage stages, of BTSC subpopulations recognizable by key traits that include epithelial cell adhesion molecule (EpCAM), leucine-rich-repeat-containing-G-pro tein-coupled receptor 5 (LGR5), and sodium iodide symporter (NIS). These identified subpopulations of BTSCs from the intramural biliary tree and that included the most primitive ones (EpCAM$^-$, LGR5$^-$, NIS$^+$) located at the base of the stem cell crypts in the peribiliary glands (PBGs); ones that are intermediates (EpCAM$^-$, LGR5$^+$ NIS$^+$) and located midway between the crypts and the bile duct lumens; and late stages (EpCAM$^+$, LGR5$^+$, NIS$^+$) ones found nearest to the bile duct lumens and also in gallbladders that have no PBGs ([1,4,29–31,33,34]). We determined that the cells we had isolated from the mice were late stage BTSCs given that they were EpCAM$^+$ (84 % ± 10.6 %), a percentage that increased up to 95 % of the cells when maintained *ex vivo* in Kubota's Medium (KM) (Fig. 1D).

Secondarily, they were characterized by immunohistochemistry staining for late-stage BTSC markers versus mature parenchymal cell markers (mAHeps), studies supporting further the conclusion that these are late stage BTSCs (e.g. such as strong staining for EpCAM and CK19) and yet with negligible expression of mature parenchymal cell genes such as albumin (ALB) and hepatocyte nuclear factor 4-alpha (HNF4α) (Fig. 1E). Gene expression patterns of day 21 BTSCs colonies further confirmed that compared to mature hepatocytes, these murine BTSCs were also positive for other endodermal stem cell markers such as Sox9 (Fig. 1F), a conclusion further confirmed by RNA-seq data comparing mBTSCs to mAHeps.

2.2. Conditions for expansion of mBTSCs

Previously, serum-free Kubota's Medium (KM) has been used for maintenance and slow expansion of human and porcine BTSCs. However, expansion of BTSCs under this condition was found to be inadequate for generating the numbers of BTSC organoids needed for future clinical programs ([3–5,13,34]). To guide our search for candidate mitogens, the mBTSCs in KM were collected for RNA-sequencing analyses to confirm the expression of stem cell-related signaling pathways when compared to those in mature, murine hepatic parenchymal cells, hepatocytes and cholangiocytes. KEGG enrichment analysis showed that primary mBTSCs have enriched stem cell-specific pathways (such as Hippo, PI3K/AKT, MAPK and Ras signaling pathways) and lack the metabolism pathways that are enriched in mature hepatic parenchymal cells (hepatocytes or cholangiocytes) (Fig. 2A).

Our previous studies of endodermal stem cells derived from embryonic stem (ES) cells and from gastric epithelia [35,36] and made apparent expansion requirements triggered by a number of small molecules (0.5 μM Bix01294, 2 μM Bay K8644, 0.04 μM RG108, 2 μM SB431542, 10 μM Forskolin, and 1 μM A83-01) and by a set of growth factors or paracrine signals (e.g. 50 ng/mL EGF, 100 ng/mL R-Spondin 1 (RSPO1), 100 ng/mL Noggin, and 50 ng/mL Wnt3a). All of these were screened on BTSC organoids and were found biologically active. This resulted in a wholly defined medium, we called 10-Defined-Proliferative-Medium (10-DPM), derived from the addition of these 10 factors to Kubota's Medium prepared with Advanced DMEM/F12 or Advanced RPMI-1640 and used for expansion of mBTSC organoids. It is called 10-DPM for the remainder of this report (Fig. 2B). The 10-DPM by itself was sufficient to maintain and expand the primary mBTSCs. After being cultured in serum-free 10-DPM for 7 days, mBTSCs appeared to have a homogeneous epithelial morphology (Fig. 2C), and the number of mBTSCs had increased significantly. By the 7th day, the mBTSCs from each C57BL/6 WT mouse in 10-DPM yielded 4.2 × 10^5 cells, about 20 times more than that in the KM condition alone ($P < 0.001$) (Fig. 2D).

Murine BTSCs, expanded in 10-DPM for 7 days, were collected for flow cytometry assays and qPCR. The overall percentagesof EpCAM$^+$ cells were maintained at 82 % ± 6.3 % (Fig. 2E). While the gene expression levels of EpCAM, NCAM and AFP of expanded BTSCs were lower, those of SOX17 were significantly higher than those of mBTSCs maintained in KM. There was no significant difference in the expression of PDX1, ICAM1 and CK19. The results showed that BTSCs cells of the P0 generation had remained hepato/pancreatic stem cells with the potential of hepatic differentiation (expressing SOX17) and pancreatic

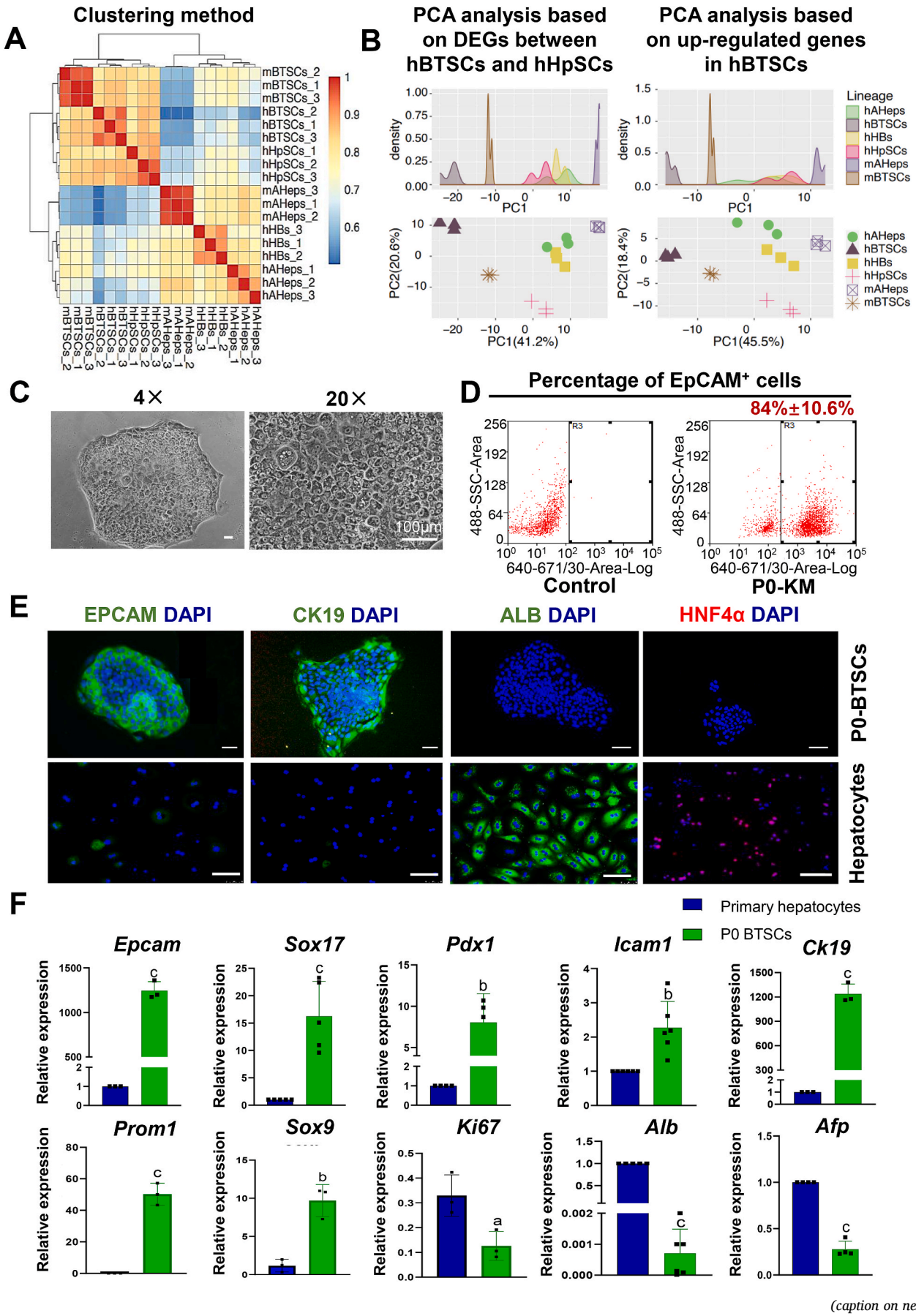

(caption on next page)

Fig. 1. Murine biliary tree stem cells (mBTSCs) in the extra-hepatic biliary tree.
(A) Correlation heat maps of mouse biliary tree stem cells (mBTSCs, 3 samples), mouse adult hepatocytes (mAHeps, 3 samples) and four, distinct subsets of human cells (hBTSCs, hHpSCs, hHBs and hAHeps, 3 samples each). The related heat maps of six types of cells showed that two main clusters were mBTSCs, hBTSCs and hHpSCs, while mAHeps, hHBs and hAHeps were clustered.
(B)Principal component analysis (PCA). The PCA analysis was processed to determine the maturational lineage stage of the mBTSCs as compared to the known stages of human hepatic and biliary stem cell maturational lineages.
(C) Morphology of primary (freshly isolated) mBTSCs cultured in Kubota's Medium (KM). Scale bar, 100 μm.
(D) EpCAM $^{+}$ proportion of cells collected from primary cultures of mBTSCs for flow cytometric sorting and analyses.
(E) Immunostaining showing stem cell markers in primary cultures of mBTSCs in KM. Scale bar, 100 μm.
(F) Expression of mBTSC genes was measured using qRT-PCR. a $p < 0.05$, b $p < 0.01$, c $p < 0.001$. Student's *t*-test.

differentiation (expressing PDX1). The proliferation ability of mBTSCs amplified by 10-DPM was better, and the differentiation potential towards liver was somewhat increased (suggested by the increased expression of SOX17 and ICAM-1), while the differentiation potential of pancreas decreased (expression of PDX1 decreased, but still higher than in the controls, and than in primary hepatocytes) (Fig. 2F). In summary, it was confirmed that mBTSCs can be expanded effectively with the 10-DPM condition with a probable enhancement of hepatic differentiation potential of mBTSCs.

2.3. Formation and passaging of mBTSC-organoids in hydrogels

Next, we attempted to passage mBTSC organoids with 10-DPM alone. We found there were very few cells that were able to re-attach to the culture surface after the enzymatic treatment of the expanded primary mBTSCs (data not shown). Therefore, we prepared two forms of hydrogels: Matrigel (Corning), used as a guide in the development of a wholly defined system, versus a hydrogel containing only defined components. For monolayer cultures, the hyaluronans could be provided as 0.05 %–0.5 % sodium hyaluronate, the water-soluble salt form of hyaluronic acid, and to which was added heparan sulfate (HS) oligosaccharides. These glycogels were marginally effective as a substratum for monolayer cultures but proved more potent when used in hydrogels into which the organoids were embedded. For the wholly defined hyaluronan hydrogels, we used Glycosil, thiol-modified hyaluronans (HA), that can be triggered with Polyethylene Glycol Diacrylate (PEGDA) to gel and, importantly, able to achieve precise levels of viscoelasticity or rigidity of the hydrogels as dictated by the ratio of Glycosil to PEGDA and with maintenance of stemness traits occurring with hydrogels at less than 100 Pa [12]. In these 3D thiol-hydrogels, mBTSCs formed organoids with a hollow structure, primarily composed of a monolayer of cuboidal epithelium. The combination of hydrogels (either Matrigel or cross-linked thiol-modified hyaluronan hydrogels) with 10-Defined-Proliferative-Medium (10-DPM) are defined as BTSC-Expansion-Glycogels (BEX-gels) and were used for the expansion of mBTSC in both monolayers (2D) and organoids (3D).

Matrigel is successful and used widely for maintenance of organoids and was used as a control to identify factors relevant to organoid maintenance and expansion and to be incorporated into a defined system. In Fig. 3A, after one day, the mBTSC organoids embedded into Matrigel could be detected under the microscope. While after 3 days, some of the organoids reached a size that was easily visualized. The organoids were cultured *ex vivo* for 5 days and expanded to a cystic structure with a diameter of 1000 μm ($P < 0.05$), with the diameter increasing nearly 6 times that of organoids on day 1 (Fig. 3A). Therefore, Matrigel proved effective for enabling expansion of mBTSC organoids proving that expansion is possible.

The immunofluorescence staining of mBTSC organoids showed that they contained cells strongly expressing markers of late-stage mBTSCs, such as those expressing EpCAM and CK19, and a marker of proliferation, Ki67 (shown as green fluorescence). DNA was labelled with DAPI (shown in blue) (Fig. 3B). The live and dead cell assays showed that most of the cells in mBTSC organoids were alive with a few being dead cells (stained as red) (Fig. 3C). Therefore, the BEX-gel system was able to maintain the mBTSC organoids. The P1 mBTSC organoids were identified by qPCR compared with the primary mBTSCs cultured in 10-DPM. Signature genes of mBTSCs indicated that they remained as hepato/pancreatic stem cells with co-expression of PDX1 and SOX17, ones that were significantly up-regulated ($P < 0.05$), and the genes remained stable before and after passaging (Fig. 3D). Comparison of P1 and P5 BTSC organoids indicated an expansion of more than 80-fold. (Fig. 3E).

We also tested the stability of mBTSC organoids expanded in the thiol-hydrogels by comparing the gene expression patterns in different generations of cells (Fig. 3F). Compared to the primary mBTSCs, the expression of EpCAM, PDX1 and Ki67 was stable in P5 mBTSC organoids. While the expression of SOX17 and CK19 increased, and the expression of PROM1 decreased in P5 mBTSC organoids. Primary (freshly isolated) hepatocytes were used as controls. Our results confirmed that the stem cell genes and proliferation ability of mBTSC organoids remained stable in the process of passaging, indicating that the defined thiol-hydrogels and the defined medium were suitable for expansion and passaging of mBTSC organoids (Fig. 3F). Although there were shifts in genes, the overall pattern indicated maintenance of those indicative of hepato/pancreatic stem cells.

2.4. Screening of essential factors of DPM for the expansion of BTSC organoids

We were interested as to which factors in the 10-DPM were the most important for the expansion of the mBTSC organoids. We carried out optimization experiments assessing the different components in 10-DPM. The paracrine signals (growth factors) and small molecular compounds were grouped into 8 clusters according to the signaling pathways in which they were involved. This was done in two phases: phase 1, assessment of the small molecules, and phase 2, assessment of the paracrine signals (growth factors).

For the small molecules, we tested the impact of omitting one small molecule at a time from the 10-DPM factors on organoid formation and gene expression levels of P1 mBTSC organoids. These included 10-DPM from which was omitted a single factor: A 83-01, Forskolin, Bix 01294, RG108, or the classical calcium channel agonist, Bay K8644. The 10-DPM was used as the positive control, while KM was used as a negative control.

Of the small molecules, Removal of RG108 from the 10-DPM set dramatically decreased the number of mBTSC organoids (Fig. 4A and B), implicating its relevance to mBTSC organoids expansion. As a DNA methyltransferase inhibitor, RG108 inhibits DNA methylation and activates the expression of genes relevant to cell proliferation. Although removal of the A83-01 and Forskolin respectively did not lead to a significant decrease in the organoid numbers (Fig. 4 B), their elimination from the 10-DPM resulted in P1 mBTSC organoids being smaller and fewer in number compared to the controls, implicating these two factors worked synergistically in expansion of BTSCs (Fig. 4C).

As an inhibitor of TGFβ kinase/activin receptor-like kinase (ALK 5), A 83-01 prevents the phosphorylation of Smad2/3 and inhibits the growth and epithelial-to-mesenchymal cell transitions induced by TGFβ. This was confirmed by the withdrawal of A 83-01 from the 5-DPM. Western blot analysis showed no significant changes in the protein expression levels of Smad2/3 in mBTSC organoids expanded in 5-DPM compared to 4-DPM (5-DPM without A 83-01) (Fig. S3C). While the

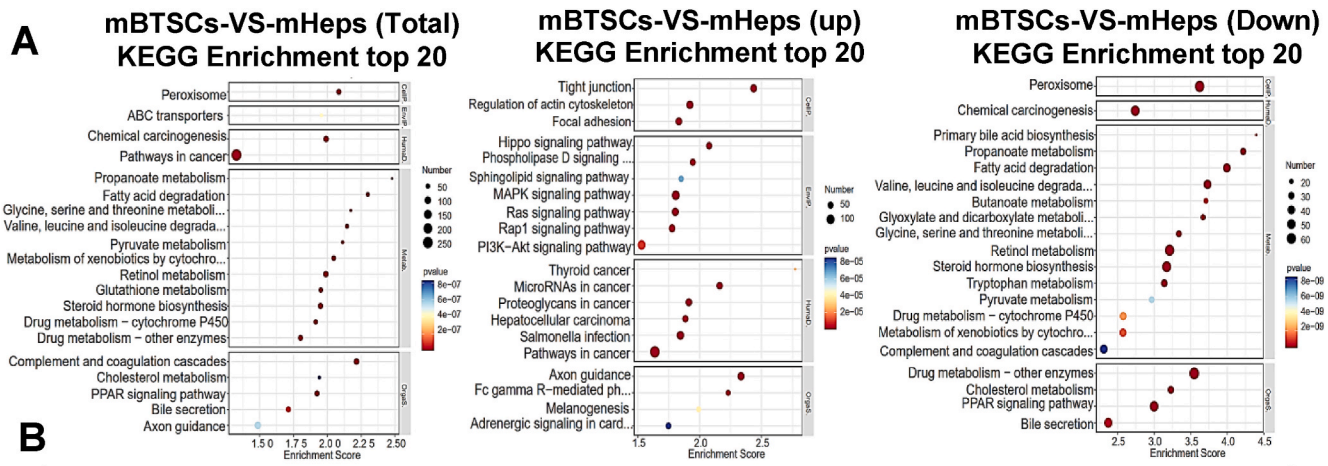

B

Name			Composition
DPM	10P	Basal Media	Advanced DMEM F12-based Kubota`s Medium
		Growth factors or hormones	50 ng/mL EGF+100 ng/mL R-Spondin1+100 ng/mL Noggin +50 ng/mL Wnt3a
		Small molecule compounds	0.5 μM Bix01294、2 μM Bay K 8644、0.04 μM RG108、2 μM SB431542、10 μM Forskolin、 1 μM A83-01
		Extra cellular matrix	A. Matrigel B. Hyaluronan (0.05% HA)+HS Extracts (100 ng/mL HSPG)

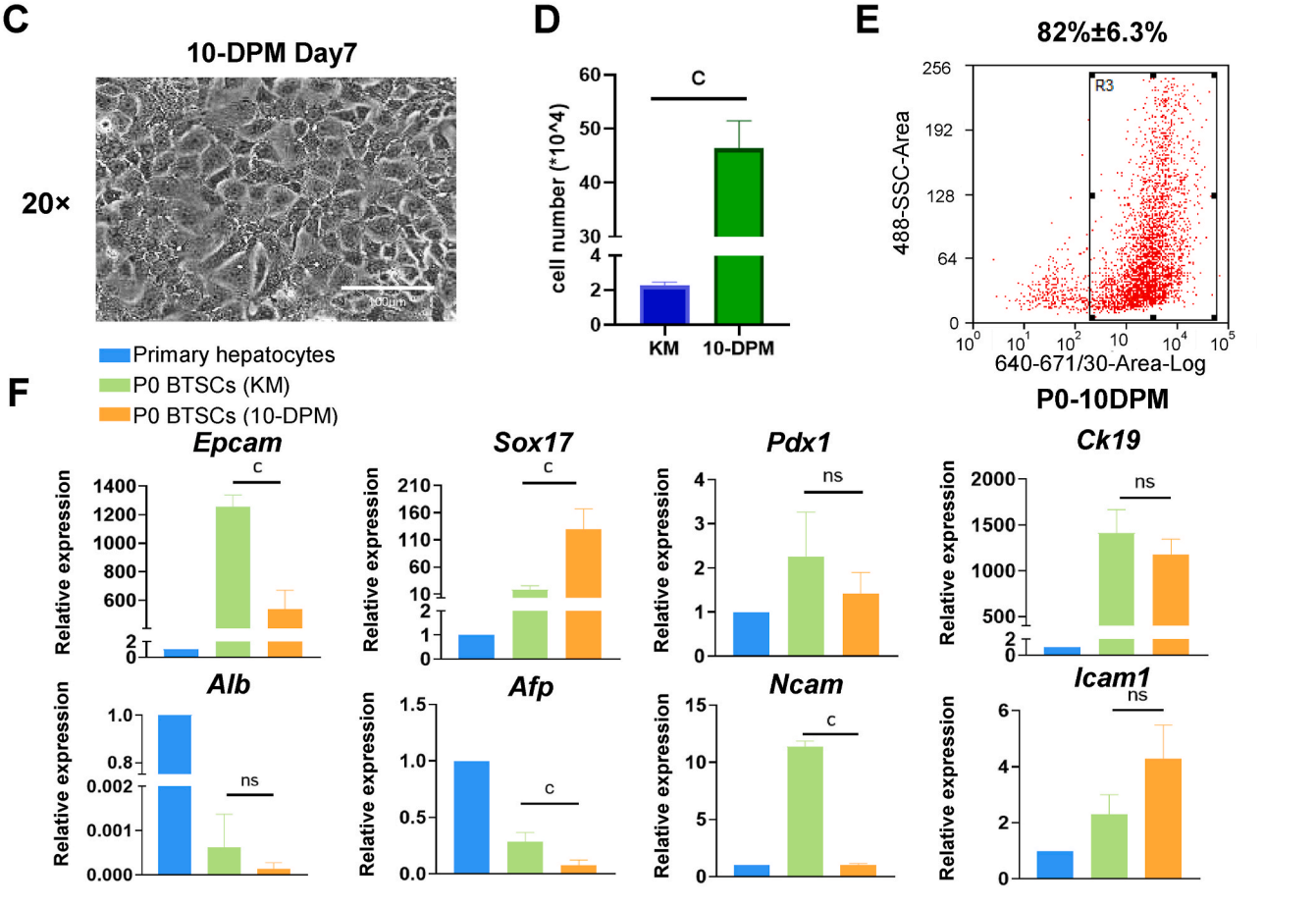

(caption on next page)

Fig. 2. Primary Culture Conditions for expansion of freshly isolated mBTSCs
(A) Differential gene expression KEGG-enrichment analysis bubble diagram (primary mBTSCs versus mature hepatocytes, mHeps); the larger the bubble, the more the number of differential protein-coding genes were evident; and the color of the bubble changed from blue to white to yellow to red. The smaller the enrichment p-value value is, the greater the degree of significance.
(B) The compositional diagram of the Glycogels in the amplification culture system of B and mBTSCs. It includes 4 growth factors and 6 small molecular compounds, abbreviated as 10-DPM.
(C) The morphology of primary mBTSCs cultured in serum-free 10-DPM on the 7th day. Scale bar, 100 μm.
(D) The number of primary mBTSCs cells isolated and cultured from each C57 WT mouse under different conditions (KM, day 21 or 10-DPM day 7). Compared with other groups, $P < 0.001$.
(E) EpCAM $^{+}$ proportion collected from primary mBTSCs in 10-DPM for flow cytometric sorting.
(F) Expression of mBTSC genes under 10-DPM condition was measured by qRT-PCR.
Data are presented as mean ± SD. a $p < 0.05$, b $p < 0.01$, c $p < 0.001$. N ≥ 3. Student's *t*-test.

expression level of Smad2/3 phosphorylation dramatically decreased in mBTSC organoids expanded in 5-DPM compared to 4-DPM (5-DPM without A 83-01) (Fig. S3D).

While Forskolin, a diterpene produced by the roots of the Indian plant, Coleus Forskohili, directly activates the adenylate cyclase enzyme, that generates cAMP from ATP, thus, increasing intracellular cAMP levels and controlling many cellular mechanisms such as gene transcription, ion transport, and protein phosphorylation.

Another relevant factor was Bay K8644, a classic calcium channel inhibitor. Removal of Bay K8644 did not result in a significant reduction in organoid numbers in Fig. 4B. However, qPCR showed that there was a decrease in the stem cell genes, PROM1 and Sox9, and in a proliferation marker, Ki67, in the cells without Bay K8644 compared to 10-DPM. Therefore, we concluded that this factor was necessary for *ex vivo* expansion and cellular stemness maintenance of mBTSCs (Fig. 4D). Taken together, we selected RG108, A 83-01, Forskolin and Bay 8644 as a 4-Defined-Proliferative-Medium (4-DPM), containing the essential small molecules requisite for expansion of mBTSC organoids.

2.5. Wnt signaling is necessary for the expansion of mBTSC organoids

Next, we tested the effect of 4-DPM on the formation of mBTSCs, where we found that mBTSC organoids maintained a small size for over a week and without sufficient proliferation (Fig. 4E and F). Therefore, we turned our attention to assessing the paracrine signals from epithelial-mesenchymal cell-cell interactions. We supplied the 4-DPM with the factors in the WNT signaling pathway (Wnt 3a and R-spondin 1/RSPO1), as well as the TGFβ signaling pathway (TGFβ protein and EGF). The results showed a significant elevation of P0 mBTSCs within 7 days whenever the WNT signals were added (Fig. 4E, Fig. S2A). The RNA-seq data also revealed that most genes related to WNT signaling pathway were up-regulated in the expanded mBTSCs compared to the primary or freshly isolated and uncultured mBTSCs and adult murine hepatocytes (Figs. S2B and S4C). We evaluated four groups using the base now defined as 4-DPM: 4-DPM + Wnt3a, 4-DPM + RSPO1 (later named as 5-DPM), and 10-DPM. The results showed that the number of P1 mBTSC organoids in 4-DPM + RSPO1 were more than that in 4-DPM, further confirming a role of the Wnt signaling pathway in cell expansion (Fig. 4F).

The P1 mBTSC organoids of 4-DPM + Wnt3a, 4-DPM + RSPO1, 4-DPM + EGF, 4-DPM + TGFβ, 4-DPM + Wnt + TGFβ groups were collected on day 5 for qPCR. As shown in Fig. S2C, the results indicated that expression levels of stem cell genes (SOX17, PROM1) and the proliferation indicator, Ki67, under the conditions of 4-DPM + RSPO1 were higher than that in the other groups (Fig. S2C). Therefore, RSPO1 was deemed necessary for expansion of BTSCs, and the 4-DPM + RSPO1 was replaced by a 5-Defined-Proliferative-Medium (5-DPM). When any one of the factors (A83-01, Forskolin, or Bay K8644) was subtracted from 5-DPM, the total number of mBTSC organoids decreased dramatically, indicating that the 5-DPM was the final optimized combination used for the expansion of the mBTSCs (Fig. S4D). Also, this 5-DPM can effectively activate the proliferation and cell cycling related pathways of the mBTSC organoids compared to the P0 mBTSCs, and as proved further by the RNA-seq analysis (Figs. S4A and B).

Interestingly, although being used widely in endodermal stem cell cultures, Wnt3a showed less effectiveness than RSPO1 in maintenance of markers of mBTSCs and in promoting the proliferation of mBTSC organoids (Fig. S2C). An explanation for this is hypothesized due to fact that the key forms of Wnts expressed in mBTSCs, in hBTSCs, and in malignant transformants of them, such as fibrolamellar carcinomas, are Wnt 4 and Wnt 7, whereas our experimental assays utilized Wnt 3a. Support for these forms as relevant in BTSCs is given also by those found to be upregulated in the expanded mBTSCs (Fig. S2B). Therefore, once Wnt 4 and Wnt 7 are available, they will need to be evaluated as ones probably relevant to BTSC organoid expansion.

Continuously, we verified the characteristics of mBTSCs we've established previously with the freshly isolated (primary) mBTSCs expanded in 5-DPM (Bix01294, Bay K8644, RG108, Forskolin and RSPO1) for 5–7 days (Fig. 4G). The immunofluorescence staining of Ki67 P1 mBTSCs organoids was done on the 7th day. Fluorescence microscopy showed that the cells expressed the proliferation marker, Ki67 (shown in green), and nuclear DNA labelled with DAPI (shown in blue) (Fig. S2E), and were found more positive than the organoids in KM. The primary mBTSCs and P5 mBTSC organoids cultured in 5-DPM were collected for qPCR (Fig. 4G). It was found that expression of BTSC stem genes were stable during passaging. As a result, 5-DPM resulted from step-by-step screening focused on the conditions required for stem cell maintenance and proliferation of mBTSC organoids *ex vivo*. We assume that additional factors might be added to this mixture once certain critical ones, such as the variant forms of Wnt, are available for testing.

2.6. The BEX-gel system enables BTSCs to minimize DNA damage during proliferation, offering protection absent in monolayers (2D systems)

Once the conditions of the expansion medium were finalized, we tested whether the system can also be used for monolayer cultures. Primary mBTSCs expanded in the 5-DPM were collected and counted after enzymatic digestion. The primary mBTSCs were re-suspended with 5-DPM. The culture plates were pre-coated with Matrigel with a concentration of (1:40) for enabling the attachment and monolayer cultures of mBTSCs. The P1 mBTSCs in monolayers yielded a homogenized cell morphology (Fig. 5A). When the cells reached 80%–90 % confluency, they were passaged at a ratio of 1:2 (the passage ratio also was determined according to the actual number of cells, for 2D, $3 \times 10^4/cm^2$; for 3D, 4000–5000 cells/10 μL); the culture medium was changed every 48 h; and the cultures were maintained for 3–5 days before passaging.

The P1 mBTSCs cultured under these conditions were collected and identified by qPCR. Compared with the primary mBTSCs cultured in 10-DPM, the expression of EpCAM, SOX17, PDX1, ICAM1 and CK19 in P1 mBTSCs in monolayer cultures (2D) proved to be stable (Fig. 5B). The gene expression observed showed no elevation of the expression of markers for endothelia (CD31) or for hematopoietic cells (CD34) (Fig. 5C). While the expression levels of AFP (a marker indicative of cells transitioning into differentiation towards liver) were increased, no albumin (ALB) was detected when compared to its expression in primary hepatocytes that were used as a control (Fig. 5B). It also showed that the

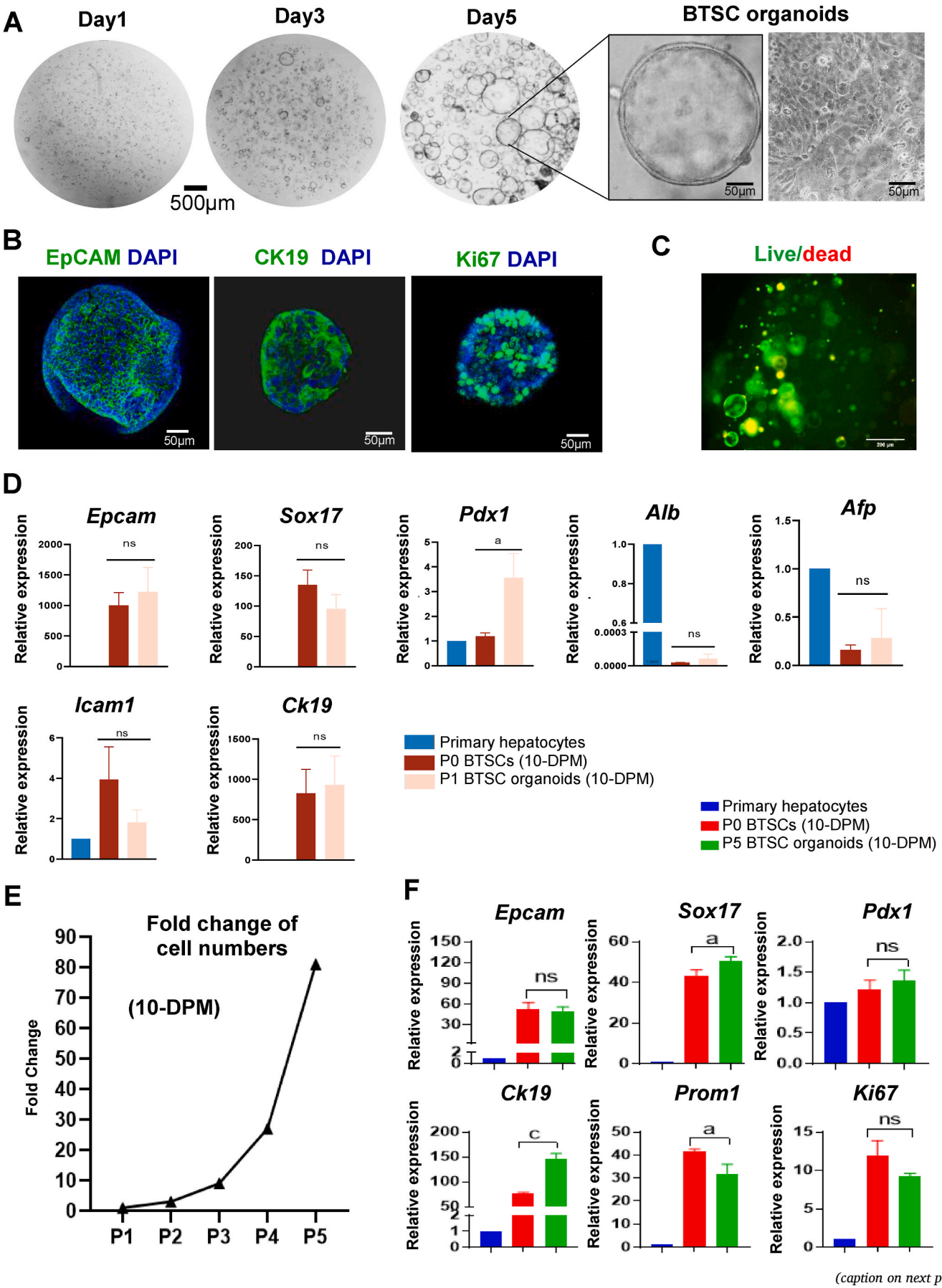

(caption on next page)

Fig. 3. Expansion of mBTSC organoids in Matrigel and in 10-DPM.
(A) The mBTSC organoids characterization formed under the condition of 10-DPM after embedding in Matrigel. Scale bar, 500 μm.
(B) Immunostained cells indicating mBTSCs traits in 10-DPM conditions. Scale bar, 50 μm.
(C) the activity and survival state of mBTSC organoids were judged by dead/live staining. Scale bar, 200 μm.
(D) Expression of the mBTSC genes under 10-DPM conditions in organoids were measured using qRT-PCR.
(E) The percentage of EpCAM $^{+}$ cells of the expanded cells during passaging. A total of 2000∼5000 cells were collected for counting.
(F) Expression of the mBTSC genes in mBTSC organoids in different generations were measured by qRT-PCR.
Data are presented as mean ± SD. a $p < 0.05$, b $p < 0.01$, c $p < 0.001$. N ≥ 3. Student's *t*-test.

level of specific stem cell genes remained stable during the passaging and expansion of mBTSCs but with a slight increase of the hepatic stem cell features. The results of cluster analysis of differential genes after transcriptome sequencing showed that the similarity of coefficients of group B (P1 mBTSCs expanded in the monolayer cultures for 5 days), group C (P1 mBTSC organoids expanded in the 3D BEX-gel system for 5 days) and group A (primary, freshly isolated mBTSCs without expansion) were higher, which proved that the cellular properties of BTSCs obtained by this expansion system remained stable (Fig. 5D).

Then, signal pathways that were significantly up regulated in the group C compared to that in the group B were investigated by KEGG. The result showed that the DNA replication-related signal pathways including DNA replication, homologues recombination and the base repair and Fanconi anemia pathways were significantly enriched in the 3D BEX-gel compared to the cells in the monolayer cultures (2D) (Fig. 5E and F). Among them, the Fanconi anemia (FA) pathway is involved in repairing DNA damage caused by endogenous and chemotherapy-induced DNA cross-linking, which indicated that the 3D culture system can promote three-dimensional expansion of BTSCs by optimizing cell DNA replication and repair function after injury. Further verification of the expression of replication protein A families (RPA), Rpa1, Rpa2, Rpa3, and RAD51 in mBTSCs cultured as monolayers and as organoids in 3D hydrogels indicating mBTSCs in the hydrogels expressed higher levels of these DNA-binding proteins that help maintain genome stability during DNA replication (Fig. 5G).

For the signaling pathways that were significantly enriched in the monolayer cultures compared to the hydrogels, stemness- and proliferation-related signaling pathways such as the PI3K-AKT signaling pathways, the MAPK signaling pathway, and the cell adhesion molecule related pathway were included in the top 20 enriched pathways (Fig. 5F). The WNT signaling pathways (Fig. S4C), and epithelial-mesenchymal transition (EMT) pathways (Figs. S4D and E) were found to be upregulated in the monolayer cultured mBTSCs compared to the mBTSC organoids (Figs. S4F and G). In parallel, we also detected the expression of histone H2AX in both mBTSC organoids expanded in monolayers versus in the 3D BEX-gel system. When DNA is attacked, especially after DNA double-stranded-breaks, serine at position 139 of histone H2AX rapidly phosphorylates, generating phosphorylated H2AX, γ-H2AX, which are commonly used to indicate DNA damage. Monolayer cultures of mBTSC organoids have more DNA damage than those in the hydrogels which might explain the poor proliferative potential of the mBTSCs in long-term monolayer cultures (Fig. 5H and I).

2.7. Heparan sulfates provide essential support of BTSCs expansion

Next, we analyzed the glycosaminoglycans (GAGs) and proteoglycans, major components in the Matrigel, with the hope that we could reconstitute a hydrogel with a defined composition. The previous studies on human BTSCs indicated that the glycosaminoglycans (GAGs) found associated with BTSCs *in vivo* or *in situ* are primarily non-sulfated ones, hyaluronans, or minimally sulfated chondroitin sulfates (CS) and heparan sulfates (HS) [26,37]. By comparison Matrigel (Corning) is composed of four major basement membrane components: laminin (∼60 %), collagen IV (∼30 %), entactin (∼8 %) and the heparan sulfate (HS) proteoglycan, perlecan (∼2–3%), but its GAGs, independent of the proteoglycan, are not yet defined [21,31.

Heparan sulfates (HS) **and heparins** (HPs), sulfated polymers of the disaccharides of GlcA or IdoA and sulfated glucosamine, are present as side chains on heparan sulfate proteoglycans (HS-PGs) and heparin proteoglycans (HP-PGs) [38,39]. The extracts of HS contain a mixture of polysaccharides carrying hundreds of different sulfated saccharide sequences. These polysaccharides bind tightly to paracrine signals, influencing their three-dimensional conformation, their binding affinities to receptors, and dictating facets of signal transduction and biological functions ([32,38,40–46]).

Therefore, we decided to test whether a combination of the 0.05 % HA and 100 ng/mL heparan sulfate proteoglycan (HS-PG) isolated from the EHS sarcoma (Sigma), was capable of supporting the expansion and passaging of the mBTSCs organoids. This hydrogel complex was named HA/HS-PG. The P0 mBTSCs expanded in 5-DPM were again collected and seeded into HA/HS-PG. The mBTSCs attached and acquired a similar growth pattern as on the Matrigel pre-coated culture plates (Fig. 6A). The expression of BTSC markers, including EpCAM, PDX1, CK19, and PROM1, were at the same level for the BTSCs expanded in HA/HS-PG and in Matrigel (Fig. 6C). While HA without the HS-PG had almost no effect on proliferation of mBTSCs, due both to poor cell attachment and also to minimal support of cell growth (Fig. 6B). Therefore, our results proved that the HS-PG is a matrix component required in our BTSC expansion system.

We further purchased commercially available heparan sulfates, an extract containing a mixture of HS oligosaccharides with distinct chemistries, from MedChemExpress (# HY-101916). We added the heparan sulfate extract into the Matrigel-based BEX-gel system. As shown in (Fig. 6D), the HS extract can significantly increase the numbers of organoids by the second day of the 3D culture. By day 3, the average diameter of organoids in the Matrigel supplied with 100 ng/mL HS was greater than in the control group with mBTSC embedded in the matrix composed only of Matrigel with 5-DPM (Fig. 6D and E). This result indicated that the HS-oligosaccharides can further improve the expansion capacity of mBTSC organoids maintained in our BEX-gel system. The gene expression pattern of mBTSC organoids expanded in the Matrigel + 5-DPM condition versus Matrigel + HS +5DMP condition further confirmed that adding HS can reduce the expression of CK19 and Sox9 of mBTSC organoids (Fig. 6F). As CK19 and Sox9 are associated with cholangiocyte differentiation of mBTSCs [37], we hypothesized that adding HS extract might be able to drive differentiation of mBTSC organoids towards cholangiocytes generated from the Matrigel + 5-DPM conditions.

2.8. Long-term expansion of mBTSC organoids maintains hepatic maturation capacity

Once the 3D BEX-gel system of mBTSC including 5-DPM and either Matrigel or HA/HS-PG + rHS3ST1 was confirmed, we further tested the stability of mBTSC organoids expanded in this BEX-gel system. We were successful in expansion of 2×10^4 primary mBTSCs isolated from the biliary tree and gallbladder to more than 1×10^9 mBTSCs by passage 20 within 70 days (Fig. 7A and B). The expression levels of EpCAM, SOX17, PDX1, AFP, CK19 were relatively stable in most for the organoids in passage 5, passage 10, passage 15, and passage 20 (Fig. 7C). The same system was also sufficient for obtaining gallbladder progenitor cells from human gallbladder. The primary gallbladder progenitor cells can

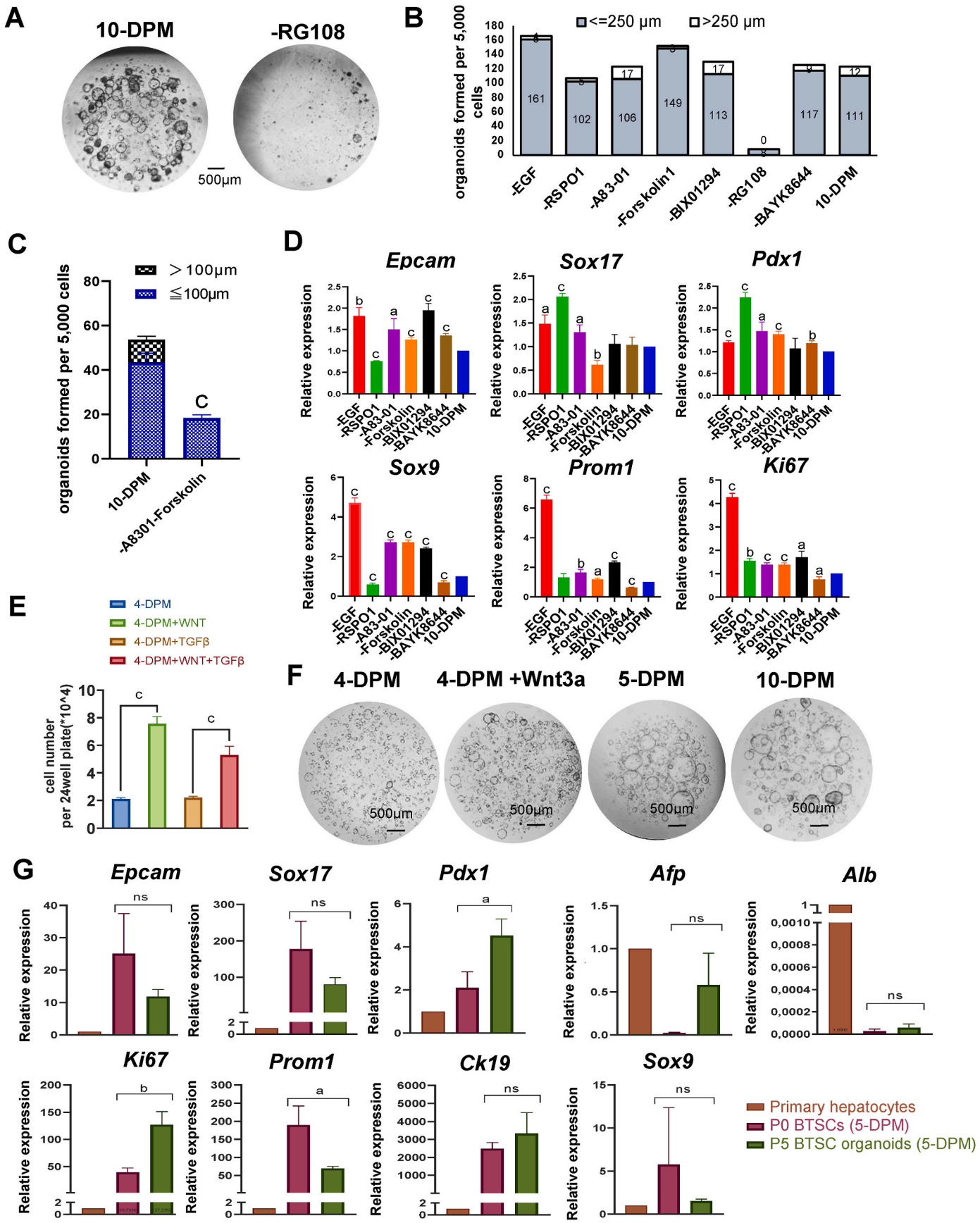

(caption on next page)

Fig. 4. RG108, A8301, Forskolin, BAY8644 are essential for the expansion of mBTSCs.
(A) Representative morphology of P1-mBTSCs organoids under the conditions of 10-DPM and 10-DPM - RG108 on the 5th day. According to the signal transduction pathways, the paracrine signals (growth factors) and the set of small molecular compounds were divided into 8 groups for screening. Scale bar, 500 μm.
(B) The number of P1 mBTSC organoids formed in each drop under 10-DPM and different screening conditions on the 5th day. The number of P1 mBTSC organoids decreased significantly under the condition of 10-DPM from which RG108 was omitted.
(C) The number of organoids formed from 5000 cells for 3 days under 10-DPM and 10-DPM - A83-01 - Forskolin. Data are presented as mean ± SD. a $p < 0.05$, b $p < 0.01$, c $p < 0.001$. N ≥ 3. Student's *t*-test.
(D) Expression of mBTSC genes in 10-DPM and other screening conditions were measured by qRT-PCR. Data are presented as mean ± SD. a $p < 0.05$, b $p < 0.01$, c $p < 0.001$, vs. 10-DPM. N ≥ 3. Student's *t*-test.
(E) Total cell number of P0 BTSCs cultured with 4-DPM + WNT signals (Wnt 3a and RSPO1), 4-DPM + TGFβ signals (TGFβ protein and EGF), and 4-DPM + WNT + TGFβ for 7 days. (RG108, A8301, Forskolin, Bay K8644 as 4-DPM). Data are presented as mean ± SD. a $p < 0.05$, b $p < 0.01$, c $p < 0.001$. N ≥ 3. One-way ANOVA.
(F) The morphology of P1-mBTSC organoids formed in 4-DPM,4-DPM + Wnt3a, 5-DPM (4-DPM + RSPO1), and 10-DPM. Scale bar, 500 μm.
(G) Expression of mBTSC genes as measured by qRT-PCR in P0-mBTSCs and P5-mBTSC organoids in 5-DPM conditions. Data are presented as mean ± SD. a $p < 0.05$, b $p < 0.01$, c $p < 0.001$. N = 3. Student's *t*-test.

form organoids in the BEX-gel system (Fig. S5), which indicated our BEX-gel system can also be used for preparation of cells from human samples.

The *ex vivo* hepatic differentiation potential of expanded mBTSC organoids was determined by placing them in an hepatic maturation or differentiation medium composed of Kubota's Medium supplemented with 0.6 mM Ca, 10^{-12} M Cu, 7 μg/L glucagon, 2 g/L D-galactose, 20 ng/mL FGF2, 20 ng/mL oncostatin M (OSM), 20 ng/mL EGF, 20 ng/mL HGF,10^{-}M/L dexamethasone, 0.1 mM/L L-Ascorbic acid, and 10 % fetal bovine serum (FBS), to achieve the conditions identified previously for lineage restriction and differentiation of endodermal stem cell subpopulations to hepatocytes [29,30,34]: After 12 days in this differentiation medium, we observed morphological changes indicative of differentiation towards mature parenchymal cells and that included ICG intake/release capacity and PAS positive staining (Fig. 7D–F).

2.9. Stem-cell-patch grafted mBTSC organoids rescued Fah$^{-/-}$ mice from tyrosinemia

The BEX-gel system was used for *ex vivo* expansion of the mBTSC organoids. When the organoids were grafted *in vivo* under the conditions used for stem-cell-patch grafting, conditions needed to enable the donor cells to express matrix metalloproteinases (MMPs) associated with stemness traits and required for engraftment and integration. Full integration was found to require both plasma membrane-associated MMPs and especially secreted MMPs and with isoforms from both epithelia and mesenchymal cells. The multiple isoforms of MMPs have been shown to be generated and are essential for the success of using stem-cell-patch grafting strategies developed previously [3,5].

In these grafting strategies, the mBTSC organoids were embedded into the thiol-hyaluronan hydrogels, prepared with Kubota's Medium, and triggered to have a rheological feature of ~60 Pa [12,47]. The grafts were used to confirm the hepatic maturation potential of the mBTSC organoids generated in the BEX-system. The patch grafts were used with donor cells derived from ZsGreen transgenic mice [5]. Gelfoam® absorbable gelatin sponges, for hemostatic use by applying to a bleeding surface, were used to replace SERI silk, used previously as a backing [3,5]. ZsGreen-mBTSC organoids were embedded in thiol-modified hyaluronan (HA) hydrogels with a rheology around 60 Pa and then were applied to both sides of Gelfoam to form a double-sided stem-cell-patch graft. The thiol-modified hyaluronan mixed with thiol-reactive polyethylene glycol diacrylate crosslinker (PEGDA) at precise ratios triggered gelation to yield a hydrogel of specified rigidity, for which that for maintenance of stem cell traits has been shown to be required to be less than 100 Pa ([3–5,12] []). The thiol-HA hydrogels provided BTSC organoids a soft mechanical force protective but yet supportive of stemness traits, avoiding rigidification during grafting. The double-sided patch graft (size of 0.4 cm × 0.4 cm) proved capable of delivering up to 3×10^6 cells/patch to the livers of host mice. The patch was inserted between the left medial and left lateral lobes of host Fah$^{-/-}$ liver and tethered at the edges by surgical glue. A distinct thiol-HA hydrogel, also prepared with Kubota's Medium, but triggered with PEGDA to have a rheology of ~200–300 Pa was applied on the serosal sides to reduce adverse reactions due to adhesions (Fig. 8A–C).

Previously, we showed that porcine BTSC organoids in stem-cell-patch grafts migrated and integrated into the liver (or the pancreas) of host organs within a week, and by two weeks had matured into functional hepatic or pancreatic cells [3,5]. We analyzed the stem cell-patch grafted livers in the host mice with an IVIS® Spectrum image system. The non-grafted Fah$^{-/-}$ mice were maintained on nitisone or NTBC [2-2-nitro-4-trifuloromethylbenzoyl)1,3cyclohexanedione] to enable them to survive their genetic condition leading to tyrosinemia. The experimental mice were transplanted with organoids of mBTSCs, using stem-cell-patch grafting strategies, and taken off the NTBC treatment; they survived and demonstrated successful engraftment of the organoids evidenced by strong green fluorescence signals (ZsGreen signals) expressed by the mBTSCs into the livers of host mice (Fig. 8D). Quantification of the intensity of ZsGreen signals between ZsGreen-mBTSCs-mice with patch grafts and wild-type mice indicated that the stem cell-patch grafting with ZsGreen-mBTSeCs showed significantly higher bioluminescence than control mice (Fig. 8E).

The liver tissues from the ZsGreen BTSC organoids that were stem-cell-patch grafted were removed and embedded into paraffin blocks to be able to detect donor cells in the host livers. The Fumarylacetoacetate Hydrolase (FAH) protein, the donor–derived hepatocyte-specific marker, was used to prove the existence of donor-derived cell engraftment in Fah$^{-/-}$ mice. When staining the livers of host Fah$^{-/-}$ mice with the FAH antibody, FAH $^{+}$ donor cells were found in the liver parenchyma, predominantly in the pericentral zones of the liver acini within 21 days after the grafting (Fig. 8F). Fah$^{-/-}$ mice receiving stem cell-patch grafts of mBTSC organoids survived for more than 2 months, while the control Fah$^{-/-}$ mice all died within a month after the withdrawal of NTBC (Fig. 8G). By 2 months, the H&E staining showed normal histological structures of grafted livers, while the IHC staining of FAH indicated that FAH $^{+}$ mature hepatocytes had been generated from the donor mBTSCs and that had fully integrated into the host liver (Fig. 8H).

Blood samples of the ZsGreen mice given stem cell-patch grafts of mBTSC organoids and the two sets of controls, the Fah$^{-/-}$ mice without the drug, NTBC, (and so succumbing to tyrosinemia), and the wild type mice, were collected for serological assays. Indicators of liver functions, including the enzymes, alanine aminotransferase (ALT) and aspartate aminotransferase (AST), were significantly improved in the experimental mice as compared to those in the control groups such as Fah$^{-/-}$ mice that were weaned from NTBC and without grafting at one month-post grafting and two month-post grafting (Fig. 8I). In summary, stem-cell-patch grafting delivered ZsGreen-BTSC organoids into the host Fah$^{-/-}$ mice within 21 days with high efficiency, and the grafted mBTSC organoids were able to improve significantly the liver functions of host mice enabling survival for at least 2 months.

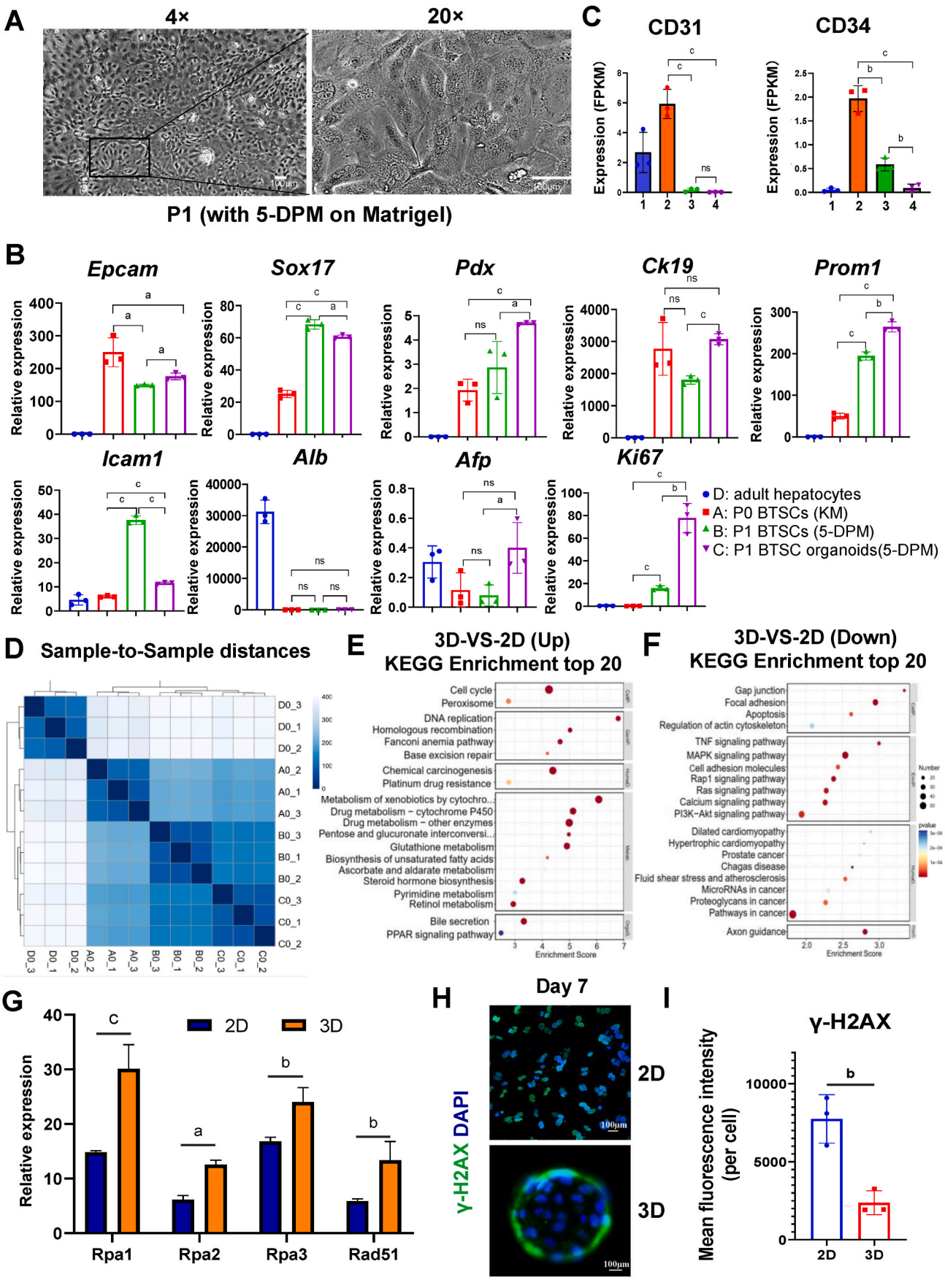

(caption on next page)

Fig. 5. Maintenance as organoids (3D) improves mBTSCs' resistance to DNA damage better than when in monolayer (2D) cultures.
(A) The morphology of P1-mBTSCs under the conditions of 5-DPM and when in Matrigel. Scale bar, 100 μm.
(B) Expression of mBTSC genes as measured by qRT-PCR in P0-mBTSCs, P1-mBTSCs, and P1-mBTSC organoids. Data are presented as mean ± SD. a $p < 0.05$, b $p < 0.01$, c $p < 0.001$. N = 3. Student's *t*-test.
(C) Expression of endothelial and hematopoietic cell related genes in cells expanded in monolayer (2D) cultures versus as organoids (3D) (RNA-seq). 1, P0-mBTSCs; 2, 2D monolayer expanded P1-mBTSCs; 3, 3D mBTSC organoids; 4. Adult hepatocytes.
(D) Sample-to-Sample cluster analysis map. The color represents the correlation coefficient.
(E) Differential gene KEGG Pathway (Up) to analyze the bubble diagram. Compared with mBTSCs expanded in monolayers (group B), signaling pathways related to DNA replication and damage repaired were significantly enriched in mBTSCs expanded as organoids (3D) (group C).
(F) Differential gene KEGG Pathway (Down) to analyze the bubble diagram. Calcium signaling pathway were highly enriched in mBTSCs expanded in monolayer (2D) as compared to BTSCs expanded in organoids (3D).
(G) Gene expression pattern of key repair factors such as RPA and Rad51 that directly act on DNA damage repair in monolayer (2D) versus organoid (3D)-cultured mBTSCs.
(H) γ-H2AX staining of monolayer (2D) versus organoid (3D) cultured mBTSCs. Scale bar, 100 μm.
(I) Fluorescence intensity statistics of γ-H2AX staining of mBTSCs cultured in monolayer (2D) versus organoid (3D).
Data are presented as mean ± SD. a $p < 0.05$, b $p < 0.01$, c $p < 0.001$. N ≥ 3. Student's *t*-test.

3. Discussion

Epithelial stem cell therapies for internal organs, such as liver, have long been desired. Early versions of fetal hepatic stem cell therapies, ones involving injection of the cells via the hepatic artery into the livers, were remarkably successful, rescuing many hundreds of patients in clinical trials in India [7–9] and in a preliminary clinical trial in Italy [6]. Two problems emerged from these clinical trials: 1) extensive ectopic distribution of donor cells in organs and tissues other than livers due to the low engraftment efficiency with donor cells delivered by blood infusion, and 2) restrictions in using fetal tissue as cell sources in many countries.

The former problem has been solved by stem-cell-patch grafting strategies that we established enabling direct transplantation of large numbers of donor BTSC organoids into the liver and yet without emboli formation or ectopic cell distribution [3,5]. The second problem has also been solved, since the requisite donor cells are found in postnatal biliary tree tissues, even in adult biliary tree tissue, that can be used as a source of BTSC organoids. What remains to enable novel cell therapy programs is the availability of sufficient numbers of BTSC organoids. Our current estimates of the number of BTSCs that can be derived from fetal or early-stage postnatal tissues (e.g. neonates) is 5×10^6, whereas a patient is estimated to require at least 5×10^7 donor cells (based on extant clinical trials) for a successful treatment. Moreover, we need to assess these expansion conditions on hBTSCs especially those derived from postnatal tissues and ideally from adult biliary trees. This is a remaining hurdle for the clinical transition of hBTSC-based therapies for the patients with liver diseases (and potentially also for pancreatic diseases).

In this study, we screened 10 factors, identified in prior reports as being relevant to expansion of endodermal stem cells ([10–12,35] [). There were three sets of factors surveyed: small molecules, various paracrine signals (growth factors), and extracellular matrix components, particularly HS-PGs and HS-oligosaccharides, and those factors were presented in monolayer cultures versus in a 3D hyaluronan hydrogel triggered to have a low rheological feature of less than 100 Pa.

Small molecule compounds and paracrine signals (RG108, A 83-01, Forskolin, BayK8644, RSPO1) promoted the expansion of mBTSC and were incorporated into a hydrogel for expansion of organoids, floating aggregates of mBTSC and their mesenchymal cell partners, precursors to endothelia and to stellate cells. The same conditions also succeeded to expand human gallbladder epithelial progenitor cells suggesting that the conditions should prove successful also for human BTSCs (Fig. S5). Thus, the establishment of this defined system to provide sufficient numbers of donor cells is a key step in translation into therapeutic clinical treatments of liver diseases.

3.1. Small molecules required for cell and organoid expansion

Small molecular compounds are key components of endodermal stem cells in *ex vivo* expansion. They comprise ones with molecular weights less than 500 Da, and ones that have been found to improve the efficiency of somatic cell reprogramming in iPSCs-related research [48–51]. Previously, we used small molecular compounds to reprogram digestive-tract-derived epithelia to obtain endodermal stem/progenitor cells [35]. These included an inhibitor of ALK4, ALK5 and ALK7 that are members of the transforming growth factor superfamily type I activin receptor-like kinase receptors (SB431542); non-ATP-competitive mitogen-activated extracellular signal-regulated kinase (MEK) inhibitor (PD0325901), the G9a-like protein and G9a histone lysine methyltransferase inhibitor (Bix01294), the non-nucleoside of DNA methyltransferase inhibitor (RG108), and the calcium Ion channel inhibitor (BayK8644). These small molecule compounds were able to replace some of the requisite paracrine signals, greatly increasing the safety and reducing the costs of stem cell expansion processes. In our study, we surveyed factors found in prior studies as candidates and that were used in a base condition of Kubota's Medium. In the initial studies, Kubota's Medium was supplemented with 10 factors, namely 10-DPM that included EGF, TGF β (A83-01, Noggin, SB431542), WNT (RSPO1, WNT3a), Forskolin, Bix01294, Bay K8644, and RG108. Wnt3a was assessed as the only form of Wnt available to us, though the forms of Wnt most strongly expressed in mBTSCs and hBTSCs and malignant transformants of them are Wnt 4 and Wnt 7.

To learn the relative importance of each of the factors, cultures were established with all 10 factors (the controls) and compared with ones in which each of the 10 factors was omitted, one by one. We found that mBTSC organoids on the 14th day of culture and treated with all 10 factors in KM were larger and more abundant than those in KM, the controls, or in those in which particular factors were omitted. Factors resulting in a reduction in the number of organoids, when they were omitted from the 10-DPM, included A83-01 or Forskolin (Fig. 4A and B). A83-01 is a TGF β Inhibitor of kinase/activin receptor like kinase (ALK 5) (IC50 = 12 nM) and can block the phosphorylation of Smad2/3 and inhibit TGF β Induced growth. A83-01 can block the phosphorylation of Smad2 and inhibit TGF-β-induced epithelial-mesenchymal transformations. In addition, A83-01 can inhibit TGF-β transcriptional activity induced by type I receptor ALK-5, activator IB receptor ALK-4, and nodular type I receptor ALK-7. Forskolin is a diterpenoid, naturally produced in the Indian plant Coleus majus, and can activate adenylyl cyclase, thus increasing the concentration of cAMP in cells [52,53]. The second messenger cAMP activates cAMP-dependent protein kinases (PKA or cAPK), regulating multiple cellular mechanisms such as gene transcription, ion transport, and protein phosphorylation. In this study, we confirmed that Forskolin and A83-01 are necessary components for *in vitro* expansion of mBTSCs in the Defined-Proliferative-Medium (DPM) of the BEX-gel system.

Other small molecules found important among those in the DPM were RG108 and Bay K 8644. RG108, is a DNA Nor-transferase inhibitor, and can inhibit DNA Nor-transferase and so activate the expression of

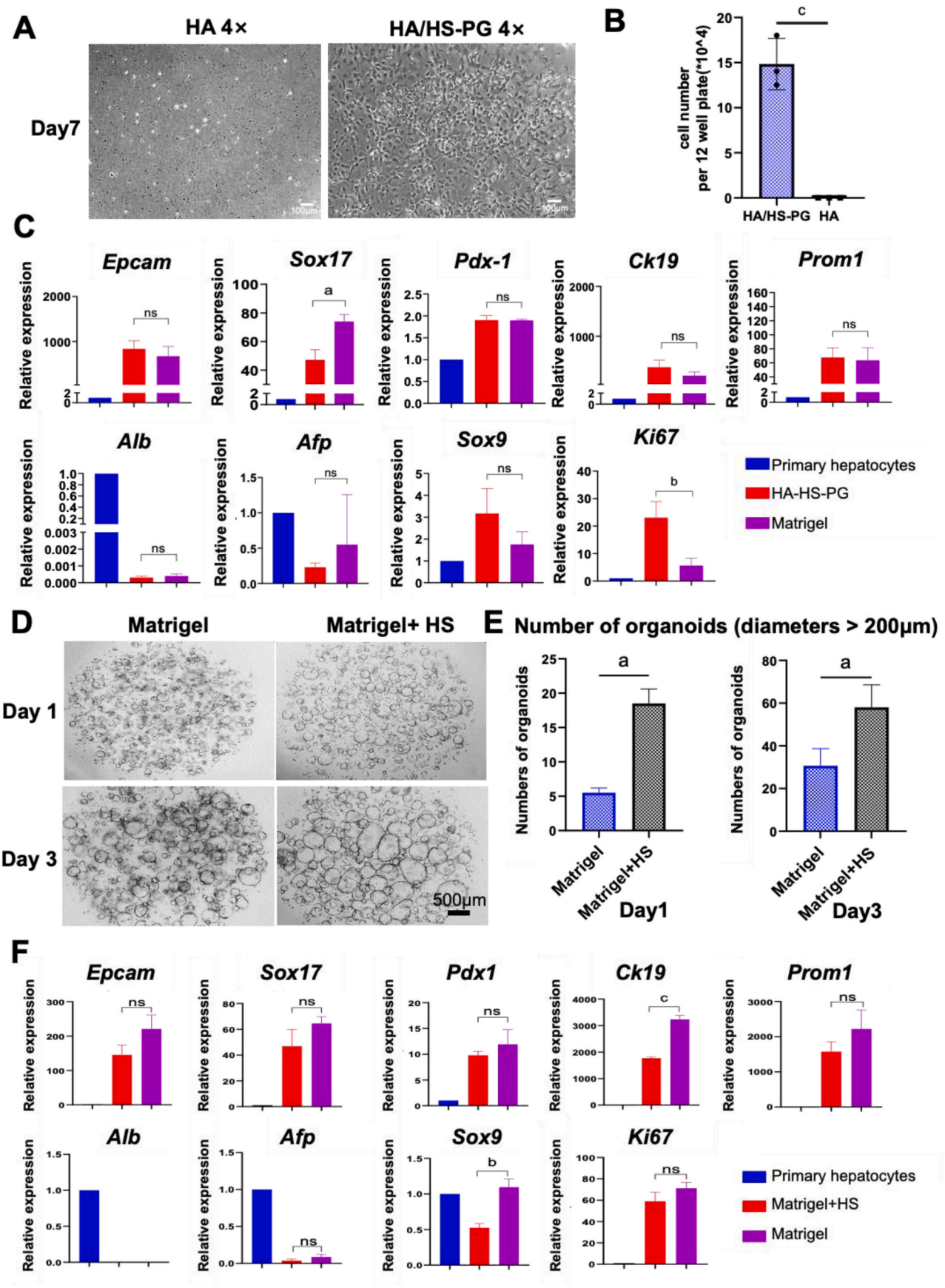

(caption on next page)

Fig. 6. Heparan sulfate in Matrigel provides support for BTSCs expansion.
(A) The morphological map of P1 BTSCs cultured in 10-DPM under the condition of serum-free 0.05 % hyaluronic acid (HA) mixed with HS-PG (Sigma) isolated from Engelbreth-Holm-Swarm mouse sarcoma, HA/HS-PG and without Matrigel. Scale bar, 100 μm.
(B) The cell number based on HA/HS-PG and HA culture conditions.
(C) Identification of gene expression levels in mBTSCs expanded in 5-DPM on the Matrigel or on HA/HS-PG-coated surface, respectively.
(D) BTSC organoids formed in Matrigel supplied with or without 100 ng/mL heparan sulfate oligosaccharides for 1 day and 3 days, respectively. Scale bar, 500 μm.
(E) Quantitative comparison of organoids formed in Matrigel only and Matrigel supplied with 100 ng/mL heparan sulfate oligosaccharides.
(F) Gene expression levels in mBTSC organoids formed in Matrigel with or without 100 ng/mL heparan sulfate oligosaccharides.
Data are presented as mean ± SD. a. $p < 0.05$, b. $p < 0.01$, c. $p < 0.001$. N = 3. Student's *t*-test.

genes related to cell proliferation, thus resulting in the proliferation of mBTSCs. BayK8644 is a classical calcium Ion channel inhibitor. These two small molecular compounds are crucial to prevent BTSCs from differentiating during expansion. The fact that the 5-DPM consists of these four small molecules with the combination of R-spondin 1 can effectively function similarly (but not entirely equivalently) to that of 10-DPM, not only reducing the cost of the expansion system, but also helping to clarify the requisite mechanisms for the *ex vivo* expansion of mBTSCs.

3.2. Monolayer cultures (2D) versus 3D ones such as organoids for stem cell expansion

Traditionally, stem cells have been expanded in monolayers on plastic culture dishes with or without coatings of matrix components. However, two-dimensional attachment on a plastic surface, even if with a matrix coating, obviates the ability of the cells to polarize fully and, of course, blocks interactions with signals on the cell surface attached to the dish or to the matrix coating on the dish. Monolayer cultures also block polarization and critical 3-dimensional platforms of antigens, ion channels and receptors at the plasma membrane, in the cytoplasm, on the nuclear membrane and in the chromatin. Cells bound to a dish, even if coated with matrix components, can experience a muting, or even fully blocking of endocytosis of factors and translocation of them to the nucleus as compared to that observed in cells in suspension and so being fully polarized. The increasing popularity of organoid cultures has fostered increasing recognition of the value of 3-dimensional cultures over monolayer ones to make feasible signaling pathways not realized previously and that are influenced by polarity.

We found that mBTSCs are more suitable for passaging in 3D BEX-gel systems than in 2D monolayers. Although mBTSC organoids can effectively proliferate in P1 and maintain high proliferative activity in BEX-gel systems, the monolayer cultures of mBTSCs had difficulties to adhere in succeeding passages. Those organoids maintained *ex vivo* in BEX-gel systems were stably passaged for more than 20 generations (Fig. 7A and B). Through transcriptome sequencing analyses, we found that organoids in BEX-gel systems have higher expression of DNA replication and DNA damage repair function signaling pathways and higher levels of the proliferation gene, Ki67, than those in monolayer cultures.

We assume that additional small molecules and/or paracrine signals will be identified that might influence the proliferation of the organoids and so our conditions should be considered as a preliminary or initial set for use. An example is that we tested Wnt3a, that did not demonstrate significant activity, but we know that Wnt3a is minimally expressed in mBTSCs. By contrast, we have yet to assess Wnt4 and Wnt7, both forms, especially Wnt7, found most abundantly in BTSCs and in their malignant transformants, fibrolamellar carcinomas. We speculate that our BEX-gel systems will likely be improved in their expansion with the addition of Wnt4 and/or Wnt 7 when those become available.

Organoids are shown to be polydispersed with a daily increasing diameter during proliferation. The sizes of organoids can vary over time both with respect to their diameters and the numbers of organoids. In our current study, we found that the organoids generated in our system are relatively uniform regardless of their size. In the future, we hypothesize the possible need to determine the most appropriate diameters of organoids during expansion to obtain the maximum numbers of cells from a single donor.

Optimizing the numbers and sizes of organoid can be achieved in background studies using techniques such as alginate encapsulation to control the size of organoids during standardized preparations of BTSC organoids [54–56]. Alternatively, we can combine our BEX-gel and DPM with microcarriers with precoated surface and proper pore size to realize the scale-up potential of BTSC or BTSC organoids with human cells for clinical applications ([57,58]). These assessments are intended to establish preparation criteria for the organoids. Ultimately, the *in vivo* studies for the final phases in preparation for clinical trials will be achieved with organoids without alginate or microcarriers and with the conditions identified from those background studies to enable rapid integration and full engraftment of the organoids now optimized for the numbers of organoids [59].

3.3. The mechanical force of hydrogels and their biological functions

The mechanical properties of the microenvironment can determine the stem cell properties via the mechano-transduction. In our previous study, we found that the hepatic stem cells isolated from the liver can maintain their stemness stage when they were embedded in the soft cross-linked hyaluronan hydrogel with a $|G^*|<100$ Pa. By contrast, increasing the rheological features of the HA hydrogel above 200–300 Pa is able to drive the differentiation/maturation of hepatic stem cells into hepatoblasts [12]. In these studies, the rheological feature of HA hydrogels was presented by the dynamic shear modulus of the HA hydrogel, [G*], where G* = G' (the elastic modulus) + iG" (the viscous modulus) and $|G^*| = [(G')^2 + (G'')^2]^{1/2}$ [12,47].

The biological effects of any biomaterials are determined by their physicochemical properties such as the biocompatibility, biodegradability, and stiffness, etc. As an important component of the stem cells niches, hyaluronans (HA) have been demonstrated in their potential to provide support for the *ex vivo* expansion of endodermal stem cells and for their engraftment *in vivo*. Hyaluronans have been the most widely used extracellular matrix components in basic research and in industry [60]. The chemical structure of hyaluronan molecules can be customized to meet the requirements of the mechanical force or time of degradation. By developing a thiol-modified HA, which can be cross-linked by PEGDA, Prestwich et al. developed the HA hydrogel with precise biochemical and mechanical properties [61]. By adjusting the ratios of HA and PEGDA solutions, HA hydrogels with the mechanical force of a range of 60 Pa to 700 Pa can be obtained from the same HA solutions [3,5,47,62–65]. In the patch grafting study, three different HA hydrogels were prepared for different purposes. The soft HA hydrogels (< 100 Pa) were used to embed the BTSCs organoids, served to prevent the maturation of BTSCs during engraftment, and were placed against the serosal surace of the target site in which the organoids were to engraft. Stiff HA hydrogels (600–700 Pa) were found to block migration of BTSCs in directions opposite to that of the target organ and were placed on the outer surface of the graft or could be replaced with a protective covering (such as the gelatin sponge used in these studies). Finally a jelly-liked HA hydrogel (~200 Pa) could be coated onto the surface of the graft (or in these studies, the sponge) and was found sufficient to miniize adhesions due to the surgical procedures.

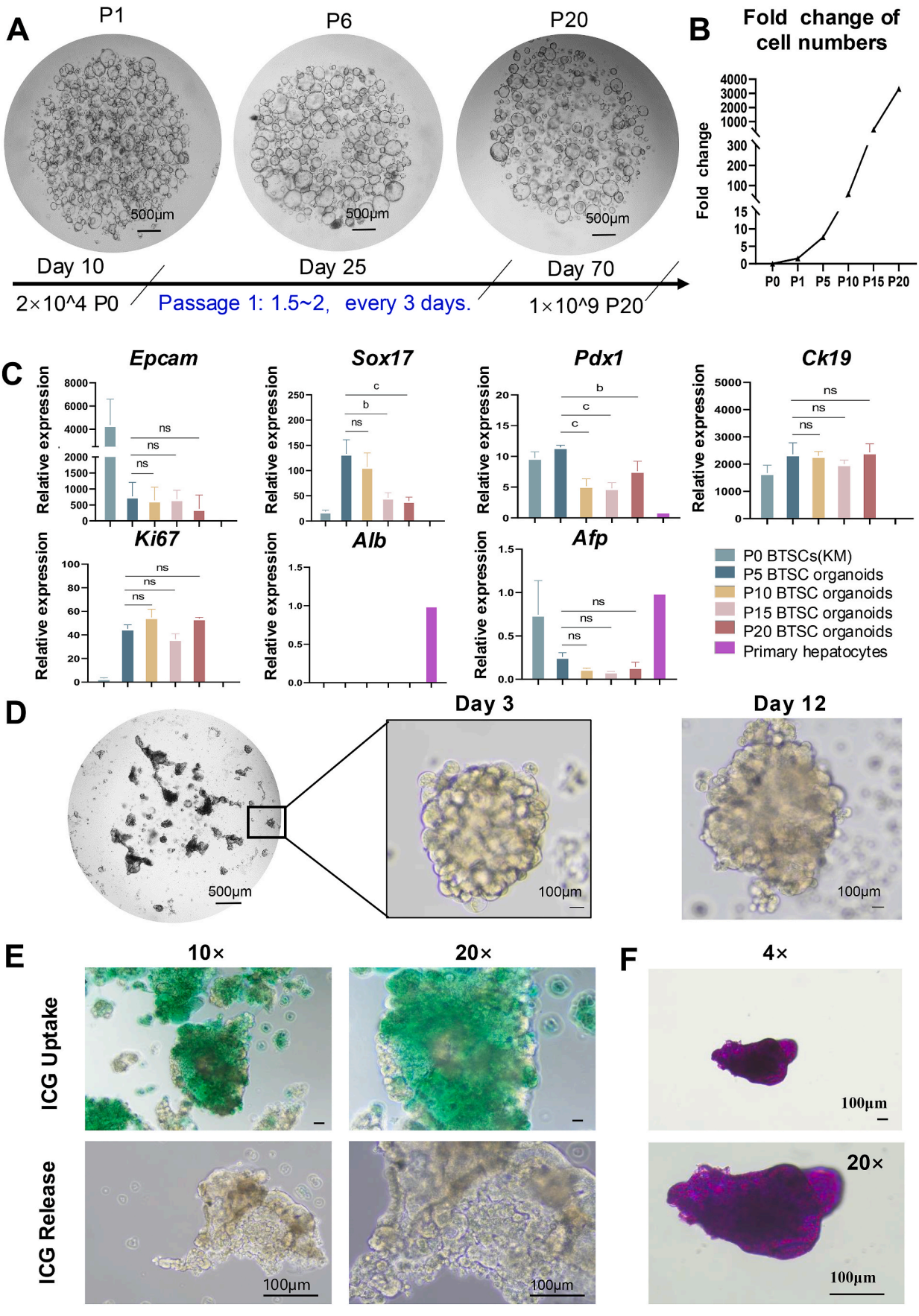

(caption on next page)

Fig. 7. Hepatic differentiation potential of expanded mBTSC organoids.
(A) Expansion of mBTSC organoids in BEX-system for 20 passages. Scale bar, 500 μm.
(B) Fold changes of total cell number of BTSC expanded in 3D system for 20 passages.
(C) Gene expression (qRT-PCR) of mBTSC-specific markers that remained stable through the passages and the expansion.
(D) The mBTSCs organoids were cultured in the expansion conditions and then tested for hepatic cell maturation for 3 days and 12 days, respectively. The mBTSC organoids transitioned into grape-shaped hepatocyte organoids.
(E) ICG intake and release of the day 12 mBTSC-derived hepatocyte organoids. Scale bar, 100 μm.
(F) PAS staining of the day 12 mBTSC-derived hepatocyte organoids. Scale bar, 100 μm.
Data are presented as mean ± SD. a $p < 0.05$, b $p < 0.01$, c $p < 0.001$. N = 3. Student's *t*-test.

Embedding organoids of stem cells isolated from neonatal livers into soft HA hydrogels and transplanted using patch grafts. The HA hydrogel provides a neutral environment during the grafting, to maintain the stem cells traits of BTSCs which retained the ability of BTSCs to secrete early-stage matrix metalloproteinases (MMPs). The secreted forms of MMPs from both the epithelial stem cells and their partners, mesenchymal cell precursors, enabled migration of organoids into the host livers within 1 week. Following the clearance of HA by the liver within 2 weeks, the donor BTSCs that had engrafted into the host liver, matured into functional hepatocytes, due to the microenvironments in the host liver and that proved able to elicit maturation of the donor organoids to a mature hepatocytes and cholangiocytes. This led to the restoration of liver functions; and so able to rescue the hosts from liver failure [3,5]. Therefore, we have demonstrated the necessity for minimal stiffness of hydrogels into which the organoids are placed for the purpose of maintaining stem cell properties. Based on these prior investigations, we combined the protocols for the BEX-gel system with those for patch grafting *in vivo* to mediate strategies for delivery of sufficient endodermal stem cell organoids into host livers.

However, since the mechanical force or stiffness of a healthy liver is approximately 6 K Pascals [66], the maturation of BTSCs into functional hepatocytes involved additional modification with other macromolecules such as collagens or gelatin [47] and other matrix components to increase the mechanical forces to meet differentiation requirements [67]. These macromolecules do not need to be added in the grafts but rather are generated by the host cells *in situ* following engraftment of the organoids and after clearance of the HA graft biomaterials.

3.4. Importance of heparan sulfate (HS) oligosaccharides

Heparan sulfate (HS) can bind to paracrine signals and other proteins that activate downstream signaling pathways by promoting the binding of paracrine signals to their receptors, or form complexes with HS proteoglycans (PGs) through heparinase cleavage to plays a role in cell proliferation and fate regulation through endocytosis and cytoplasmic signaling transduction. The effect of the complexes of [paracrine signal-a specific HS oligosaccharide] depends on both the biological activity of the paracrine signal and the complexes as a whole. In our study, by replacing Matrigel with mixtures of hyaluronans and extracts of heparan sulfate oligosaccharides from Matrigel (referred to as HA/HS), there was continued expansion of BTSC organoids. As a complex network structure of protein and polysaccharides secreted and assembled by cells, extracellular matrix (ECM) provides attachment sites and structural support for cells and enables the surface and intracellular antigens, ion channels, receptors and other cellular components to be in a configuration optimal for growth versus differentiation responses.

The biological activity of HSs primarily depends on their sulfation patterns on the GlcA or IdoA and includes distinctive patterns of N-sulfation and *O*-sulfation such as 2-*O*-HS, 3-*O*-HS and 6-*O*-HS. Parallel studies assessing the biological effects of synthesized forms of HS-oligosaccharides on organoids of human hepatic stem cells indicated an importance of 3-*O*-sufated heparan sulfates for both human BTSCs and for fibrolamellar carcinomas, malignant transformants of hBTSCs [31]. Our bioinformatic analyses indicated that 3-*O*-sulfotransferase-related genes are also enriched in hBTSCs, where the 3-*O*-sulfotransferases are responsible for the synthesis of 3-*O*-sulfated HS-oligosaccharide. Therefore, we investigated the expression of sulfotransferases genes in our murine BTSCs' RNA-seq data (Fig. S6). The RNA-seq data were further verified with that from qPCR. The results showed that among the seven subtypes of HS 3-*O*-sulfotransferases (HS3STs) (HS3ST1, 2, 3A, -3B, -4, -5 and -6), the HS3ST1 subtype is highly expressed in mBTSCs (Fig. S6).

HS-3-*O*-sulfation is a rare modification isoform of HS-oligosaccharides. The HS-oligosaccharides from endothelial cells contain about one 3-*O*-sulfate group per 100 disaccharides [68]. By contrast, the basement membrane HS-oligosaccharides from the EHS sarcoma, from which Matrigel is prepared, does not contain any 3-*O*-heparan sulfate oligosaccharides [69,31,70]. We have recently established a technology that can analyze picograms of heparan sulfate [71,72], testing for the contents of 3-*O*-HS-oligosaccharides and other HS-oligosaccharides in Matrigel and other extracellular matrix materials that are candidates for the expansion of BTSCs.

Most importantly, we have not yet tested the available synthesized forms of 3-*O*-HS-oligosaccharides of defined length (10-mers to 18-mers) found to be biologically active on human hBTSC and hHpSC organoids (Zhang W et al, manuscript in preparation). These are now commercially available from Glycan Therapeutics (Raleigh, NC) as synthesized forms of 3-*O*-HS-oligosaccharides. These will be assessed to optimize further the conditions for expansion of the organoids to be used for the clinical applications. Other studies assessing the roles of 3-*O*-HS oligosaccharides have shown their ability to promote expansion of KIT $^+$ progenitor cells in the salivary glands by affecting the binding affinity of FGF to receptors [73]. Therefore, 3-*O*-sulfated HS-oligosaccharides will be assessed in future studies.

4. Conclusions

BTSCs, co-hepato/pancreatic stem cells, have been identified in multiple mammals including humans and pigs ([4,34,37]), and in this study, also in mice. Human biliary tree stem cells (hBTSCs) have shown their translational potential in cell therapies of liver and pancreatic diseases including diabetes [6,74]. Preparation of sufficient number of BTSCs from limited donor organs is a crucial step for transitions into clinical programs of cell therapies with organoids of hBTSCs. In this study, we have established a Defined-Proliferative-Medium (DPM) consisting of four small molecules (RG108, A 83-01, Forskolin and BAY8644) and R-spondin 1 (a member of the Rspo family of Wnt modulators) for the expansion of mBTSCs. Transplantation of mBTSC organoids prepared in this DPM and embedded in soft hydrogels (< 100 Pa) facilitated engraftment of mBTSC organoids that had been passaged for more than 20 passages (> 3000 fold). The conditions proved crucial in maintaining the stem cells traits of mBTSCs and in their engraftment into host livers.

It is expected that the BEX-gel system conditions will be improved potentially with the addition of other factors, the most likely being other forms of Wnt plus synthesized forms of important HS-oligosaccharides. In parallel, the conditions will be characterized further for those facilitating maintenance of BTSC subpopulations with preferential linkage towards hepatic versus pancreatic fates and/or those enabling maintenance of the very primitive BTSCs with sustained potential for both hepatic and pancreatic fates. These should greatly facilitate the ability to use BTSC organoids in the next stages of research such as testing these

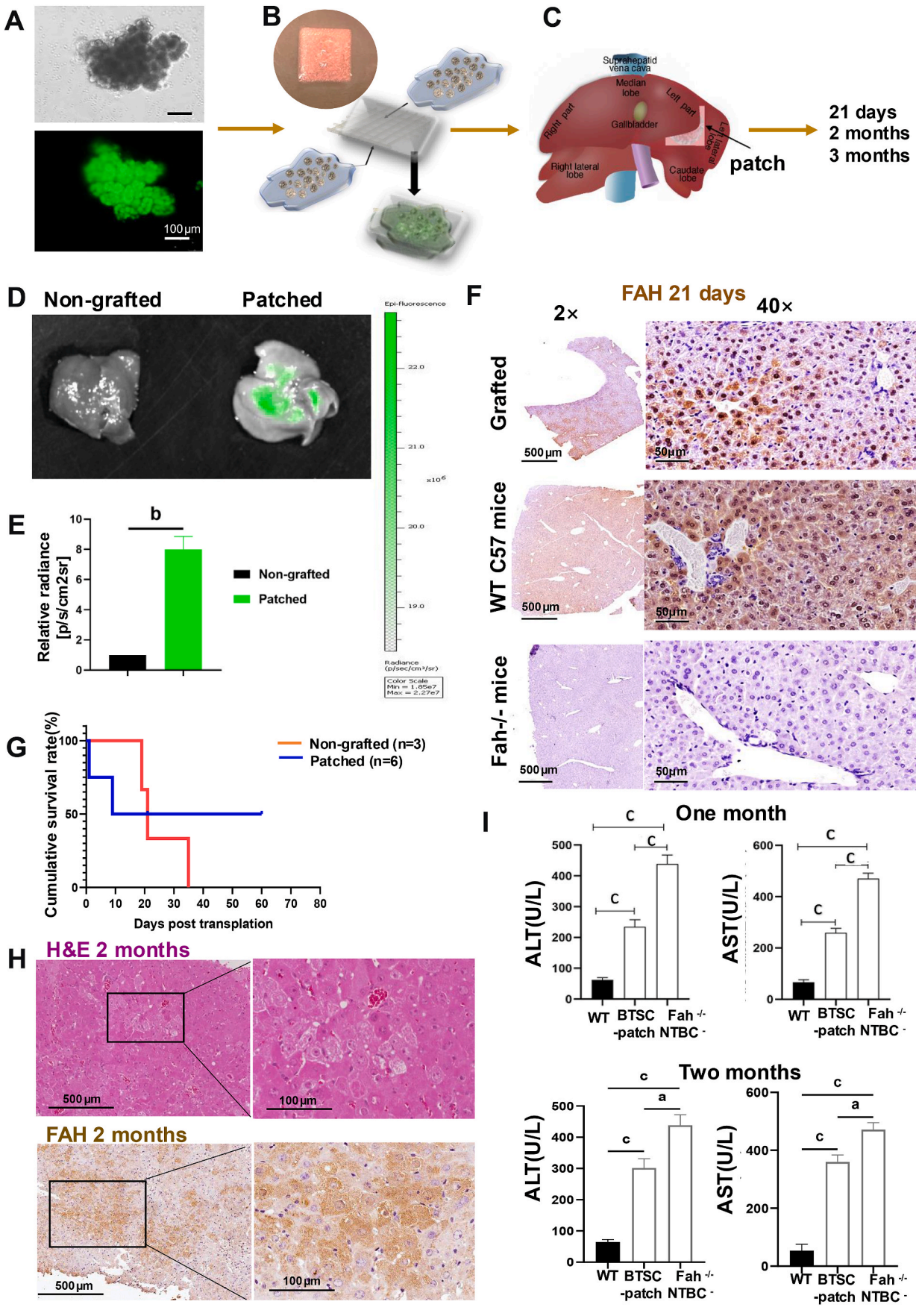

(caption on next page)

Fig. 8. Stem-cell-patch grafting of mBTSCs organoids into mice with liver failure.
(A) Morphology of ZsGreen mBTSC organoids containing mBTSCs under bright field and with green fluorescence. Scale bar, 100 μm.
(B) The mBTSCs organoids were embedded in stem-cell-patch grafts comprised of thiol-hyaluronan hydrogel prepared with Kubota's Medium and triggered to gel with PEGDA to a level of viscoelasticity of less than 100 Pa. The stem-cell-patch graft tethered to the liver was protected with a covering of a gelatin sponge.
(C) The mBTSC organoids embedded in the thiol-hydrogel prepared with Kubota's Medium was used as a stem cell-patch graft placed between the median lobe and left lateral lobe of the $Fah^{-/-}$ mouse. Surgical glue was applied at the edges of the graft to tether it to the site.
(D) A $Fah^{-/-}$mouse with a stem cell-patch graft of ZsGreen-mBTSC organoids and a wild-type mouse were placed in IVIS® Spectrum CT instrument for detecting the level of intensity of ZsGreen.
(E) The intensity of the ZsGreen signal of livers and spleens of stem cell-patch grafted $Fah^{-/-}$ mouse and wild-type mouse were detected instantly after detachment. Values of ZsGreen intensity in the liver and spleen of grafted mice and control were compared.
(F) IHC staining of FAH of $Fah^{-/-}$ host mice liver grafted with ZsGreen BTSC organoids for 21 days. Liver tissues from wild type mice and $Fah^{-/-}$ mice were used as positive and negative controls. Scale bars represent 500 μm (images with lower magnification) and 50 μm (images with higher magnification).
(G) The comparison analysis of survival curves of patch grafted $Fah^{-/-}$ host mice versus non-grafted $Fah^{-/-}$ host mice after the NTBC withdrawal,
(H) H&E staining and IHC staining of FAH for $Fah^{-/-}$ host mice at 2 months post-grafting. Scale bars represent 500 μm (images with lower magnification) and 100 μm (images with higher magnification).
(I) Liver functions of alanine aminotransferase (ALT) and aspartate aminotransferase (AST) in wild type (WT) mice, in mBTSC-organoid-patch grafted $Fah^{-/-}$ mice (no NTBC), and in liver injury $Fah^{-/-}$ mice due to the withdrawal of NTBC (control). Blood samples were collected at 1 month and 2 months-post grafting for this assay. Data are presented as mean ± SD. a. $p < 0.05$, b. $p < 0.01$, c. $p < 0.001$. $N = 3$. Student's *t*-test.

conditions on human BTSC organoids. Ultimately, the expanded organoids prepared *ex vivo* will be evaluated in translational studies *in vivo* leading to clinical programs of stem-cell-patch grafting of BTSC organoids *in vivo* for treatment of hepatic and pancreatic diseases.

5. Methods

5.1. Companies

Abcam (Cambridge; England); **Abmole** (Houston, TX; USA**; Bimake** (Houston, TX; USA); **Biolegend** (San Diego, CA; USA); **Biotime** (Alameda, CA; USA); **Corning** (New York, NY; USA); **GIBCO/Invitrogen** (Shanghai; China); **MCE** (Monmouth Junction, NJ; USA) **PeproTech@-Thermofisher** (Cranbury, NJ; USA)); **R&D Systems** (Minneapolis, MN; USA); **Sangon Biotech** (Shanghai; China); **Shanghai Jihui Experimental Animal Breeding Company** (Shanghai; China); **Sigma-Aldrich** (St. Louis, MO; USA); **Takara Bio** (Kusatsu, Shiga; Japan); **Selleck** (Houston, TX; USA); **Vesta Biotherapeutics** (Branford, CT; USA).

5.2. Tissues and ethics approvals

Human gallbladder and cystic duct. Based on the anatomical structure of the human biliary system and the feasibility of obtaining clinical specimens, we determined that the gallbladder and the cystic duct tissues which are commonly discarded after surgery, were used as the source of human BTSCs. The use of human tissue was approved by the human subject review committee in Shanghai East Hospital Affiliated to Tongji University. Authors complied with all relevant ethical regulations, and written consent has been obtained from all patients.

Animals. All animal use was in accordance with the guidelines of the Ethical Committee of Experimental Animal of the Tongji University. The experimental procedures were approved by the Ethical Committee in Shanghai East Hospital Affiliated to Tongji University. C57BL/6 WT mice and $Fah^{-/-}$ mice were maintained in the animal facilities of Shanghai East Hospital (Shanghai, China). C57BL/6 mice were purchased from Shanghai Jihui Experimental Animal Breeding Co., Ltd.

5.3. Media and solutions

All media were sterile filtered (0.22 μm filter) and kept off the light at 4 °C before use. Basal medium and fetal bovine serum (FBS) were purchased from GIBCO/Invitrogen.

Cell Wash. 500 mL of basal medium (RPMI 1640; Gibco # C11875500BT) was supplemented with 0.5 g of serum albumin (Sigma, # A8896-5G, fatty-acid-free), 10^{-9} M selenium, and 5 mL of Antibiotic-Antimycotic (Gibco #15240-062, AAS). It was used for washing tissues and cells during processing.

Collagenase solution. Consists of 100 mL of cell wash supplemented with collagenase (Sigma # C5138) with a final concentration of 600 U/mL (R1451 25 mg) for biliary tree (ducts) tissue and 300 U/ml (12.5 mg) for organ (e.g. liver) digestion.

Kubota's Medium [10,31]. A wholly defined, serum-free medium designed originally for hepatoblasts, and then found successful for biliary tree stem cells, hepatic stem cells, pancreatic stem cells, lung stem cells and, with minor modifications, for intestinal stem cells. Thus, in general, it is useful for endodermal stem/progenitors and was used to prepare cell suspensions, organoids and HA hydrogels. This medium consists of any basal medium with no copper, low calcium (0.3 mM), 1 nM selenium, 0.1 nM zinc sulfate heptahydrate, 4.5 mM nicotinamide, 0.1 % bovine serum albumin (purified, fatty-acid -free; fraction V), 10 μg/mL transferrin/Fe, 5 μg/mL insulin, 10 μg/mL high density lipoprotein, and a mixture of purified free fatty acids that are presented complexed with fatty acid-free, highly purified albumin. Its preparation is given in detail in a method review [75]. It is available commercially from Vesta Biotherapeutics (Branford, CT).

We used Kubota's Medium as a base prepared in advanced DMEM/F12 as the basal medium, conditions demonstrated previously to support long-term stability and expansion of endodermal stem cells isolated from every mammal assessed (mice, rats, pigs, humans) ([3–5,10]). It was supplemented with the growth factors (paracrine signals) and small molecular compounds as needed for this study to yield expansion of mBTSCs (see Fig. 2B). These included 4 growth factors (EGF, R-Spondin1, Noggin, and Wnt3a), and 6 small molecule compounds (Bix01294, BayK8644, RG108, SB431542, A83-01, Forskolin), which were prepared as a mixture called 10 Defined-Proliferative-Medium (10-DPM). The final composition of the expansion conditions iincluded A83-01, BayK8644, RG108, Forskolin and R-Spondin1 and was named 5-DPM.

5.4. BTSCs isolation

Extrahepatic biliary tree tissues (including the gallbladder) were isolated from C57BL/6 WT mice. The biliary tree was first washed with the "cell wash" buffer comprised of a sterile, serum-free basal medium supplemented with antibiotics, 0.1 % serum albumin, and 1 nM selenium (10^{-9} M). It was then mechanically dissociated with scissors, and the aggregates enzymatically dispersed into a cell suspension in RPMI-1640 supplemented with 0.1 % bovine serum albumin (BSA), 1 nM selenium, 300 U/mL type IV collagenase, 0.3 mg/mL deoxyribonuclease (DNAse) and antibiotics. Digestion was done at 37°C with frequent agitation for 15 min. This was followed by centrifugation at 1000 rpm at 4°C. The cell pellets were again re-suspended in cell wash and filtered through a 40 μm nylon cell strainer and with fresh cell wash. Next, the cell pellets were subjected to centrifugation at 800 rpm and at 4°C to remove the supernatant. The cells were re-suspended in the KM with 5 %

fetal bovine serum and inoculated into the culture plates for adherent cultures to grow overnight. The next day the medium was replaced with serum-free KM or with 10-DPM or 5-DPM. Fresh medium was provided every 2–3 days. Primary cells were collected for sub passaging cultures at day 7.

5.5. BTSCs expansion

During passaging, the primary culture medium used for BTSCs was removed; the cells were digested with TrypLE (GIBCO, 12604021) at 37°C, and every 3 min the cells were agitated strongly. Then advanced DMEM/F12 was added to stop digestion. The cell numbers were determined, and viability was assessed using Trypan Blue exclusion assays.

1 Passaging of monolayer mBTSCs cultures (Two-dimensional–2D)

After counting, the BTSCs were plated onto culture plates pre-coated with 2.5 % Matrigel and cultured at 37 °C, in a 5 % CO_2 incubator until cells reached 80 %–90 % confluence. The medium was changed every other day. Cells were passaged at a ratio of 1:2 (the passage ratio was determined to correlate the actual number of cells after counting), and the culture medium was changed every 2–3 days.

Alternatively, the cells were cultured in the mixture of hyaluronans supplemented with HS-PG (Sigma). The 10-DPM was mixed with HS-PG and 0.05 % Hyaluronan to replace the Matrigel. The cultures were provided with medium changes every 2–3 days.

2. Passaging of mBTSCs organoids (three-dimensional passaging–3D)

In order to obtain BTSCs organoids, cells and Matrigel were mixed 1:1 and dropped onto culture plates as 4000–5000 BTSCs per 10 μL. The cell culture plates were placed upside down in the incubator. After the Matrigel droplets solidified, the culture plates were placed in the normal orientation and covered with 10-DPM or 5-DPM.

With passaging, the culture medium of the BTSC organoids was removed. BTSC organoids were digested with TrypLE (GIBCO, 12604021) at 37 °C. Matrigel droplets were mechanically dispersed by pipetting the TrypLE to break the organoids to obtain cell aggregates of up to 10 cells (these are visible under microscopic observation). The digestion medium was diluted with the culture medium to stop the dissociation. Cell clusters were then counted and embedded in the matrix to form organoids.

5.6. Hepatic differentiation medium

Kubota's Medium was prepared with calcium to achieve a concentration of 0.6 mM Ca, and then was supplemented with 10^{-12} M Cu, 7 μg/L glucagon, 2 g/L D-galactose, 20 ng/mL FGF, 20 ng/mL oncostatin M (OSM), 20 ng/mL EGF, 20 ng/mL HGF,10^{-7}M/L dexamethasone, 0.1 mM/L L-Ascorbic acid, and 10 % fetal bovine serum (FBS). The mBTSCs were induced for 12 days in the hepatic differentiation medium before running the qPCR-detection analyses.

5.7. Quantitative reverse transcription and polymerase chain reaction (qRT-PCR)

Total RNA was extracted from the organoids or grafts using Trizol (Invitrogen). The cDNA was synthesized using PrimeScript™ RT Master Mix (Perfect Real Time) (Takara Bio Inc., Shiga, Japan) that was used as a template for PCR amplification. Primers were obtained from the primerbank (https://pga.mgh.harvard.edu/primerbank/) and synthesized by Sangon Biotech (Shanghai, China). Mixtures were annealed at 50 °C for 2 min and 95 °C for 10 min, followed by 40 cycles at 95 °C (5 s) and 60 °C (34 s). Expression of glyceraldehyde-3-phosphate dehydrogenase (GAPDH) was used as a control. Standard Primers are listed in Supplementary Table S2.

5.8. Preparation of primary murine hepatocytes

The digestion buffer was prepared, and the final concentration of collagen IV was 0.3 mg/mL. We prepared 50 mL of digestion buffer consisting of 49.5 mL EBSS (Earle's Balanced Salt Solution, Gibco, 24010), 0.5 mL HEPSS (4-Hydroxyerhylpiperazine-1-propanesulfonic acid Buffer Solution, Gibco, 15630) and 0.03 g collagen IV.

The mice were anesthetized using an intraperitoneal injection of tribromoethanol (final concentration-350 mg/kg). The inferior vena cava was cannulated, and the liver perfused to remove the blood and circulating cells by means of the perfusion medium of EBSS and HEPSS (50 mL liver perfusion medium, EBSS 49.5 mL + HEPES 0.5 mL). While the buffer was running through the needle, the needle was inserted into the vena cava. Immediately upon appearance of white spots and/or portal vein swelling, the portal vein was cut with scissors. The needle was removed before air was able to get into the liver. The liver was dissected and removed gently using forceps to grab the central connective tissue between the lobes. Then the liver connections to other organs were remove; the gall bladder was removed; and the liver was placed in the digestion buffer and put on ice. The liver surface was ruptured with fine tip forceps, and the cells were gently released. The cells were filtered as 5 mL of cell suspension through a 70 μm cell strainer into a 50 mL tube. The cells were then spun down at 1000 rpm/min for 5 min at 4 °C. The supernatant was aspirated, and 5 mL of DMEM media was added. Cell viability was determined with cell counts in a sample assessed with trypan blue. Cells were plated evenly across the plates or wells and then put into a humidified CO_2 incubator. After 2h, the medium was changed, and this was repeated after 24h.

5.9. Hepatocyte functional analysis

ICG-uptake and release: ICG powder (Tsbiochem, T14875) was prepared in sterile, ultrapure water to a final concentration of 5 mg/mL. Before use, the ICG storage solution and culture medium were diluted into working solution according to the ratio of 1:4. The induced cells were washed with PBS and indocyanine green working solution was added. The cells were then incubated in a 5 % CO_2 incubator at 37 °C. The above solution was discarded, and the working solution thoroughly washed off with PBS. The normal medium was added. Under the microscope, green granules were observed in the cytoplasm of cells ingested with ICG granules. After incubating at 37 °C and in 5 % CO_2 for 1 h and 2 h, the image of ICG release was analyzed under microscope.

PAS staining: Done according to the manufacturer's instructions; the cells were stained with Periodic-Acid-Schiff (Beyotime, C0142S). The stained cells were washed by PBS and fixed at room temperature with 4 % PFA. After 10 min, the cells were washed, and periodate solution was added. Schiff staining solution was added to each sample after rinsing, and the dye solution was removed after avoiding light at 37 °C for 30 min to 1 h. Then hematoxylin was added to each sample. The samples were washed for 30 s until the color that was floating (not bound to the cells) was washed away.

5.10. Immunofluorescence

The cells were incubated in 4 % paraformaldehyde (dissolved in PBS, pH 7.4) for 10 min at room temperature. The cells were washed in PBS three times for 5 min. The samples were then incubated with PBS (including 0.25 % Triton X-100) for 15 min. Cells were incubated with 1 % BSA for 45 min at room temperature. Primary antibody was prepared on ice and incubated in the humidifying box at 4 °C overnight. Cells were then washed in PBS three times for 5 min. Secondary antibodies were incubated at room temperature in the dark for 45 min. After washing in PBS three times, each time for 5 min, 1 × DAPI was added. The cells were covered with cover slips. A Leica automatic fluorescence microscope was used to observe and take pictures. The antibodies used are listed in Table S1.

5.11. Cell preparation for RNA-Seq

In this experiment, 12 samples, including primary murine hepatocyte, P0 mBTSCs (in KM)、P1 mBTSCs (in 5-DPM), P1 mBTSC organoids (in 5-DPM), were submitted to OEbiotech (Shanghai, China) for RNA-sequencing. After extracting the total RNA of the samples and digesting the DNA with DNase, the mRNA was enriched with magnetic beads containing Oligo (dT), and the mRNA was converted into short fragments by adding an interrupting reagent. Using the interrupted mRNA as a template, a six-base random primer was used to synthesize one-stranded cDNA, and then a two-strand synthesis reaction system was prepared to synthesize two-stranded cDNA, and the double-stranded cDNA was purified using a kit. The purified double-stranded cDNA was then end-repaired, A-tailed, and sequencing adapters were ligated, followed by fragment size selection, and finally PCR amplification. After the constructed library was qualified by the Agilent 2100 Bioanalyzer, Illumina HiSeq X Ten sequencer was adopted to generate 150 bp paired-end data (raw data).

5.12. RNA-seq-data analysis

In view of the influence of the data error rate on the results, fastp software was used to perform quality preprocessing on the raw data, and the number of reads during the entire quality control process was statistically summarized. For each sample, we used hisat2 to compare CleanReads with the specified reference genome, obtain position information on the reference genome or gene, and sequence feature information specific to the sequenced sample. We use htseq-count software to obtain the number of reads aligned to protein-coding genes in each sample. The FPKM value was calculated for the gene expression levels.

5.13. Correlation analysis

The correlation between samples/lineage cells reflects the degree of similarity between samples/lineage cells. The closer the correlation coefficient is to 1, the higher the similarity between samples/lineage cells and the smaller the difference between samples/lineage cells. We used the previously obtained FPKM data of mouse lineage cells and similar data of our previously known human lineage cells (GSE73114, https://www.ncbi.nlm.nih.gov/geo/) as an input file for correlation analysis using R. Then, we calculated the correlation coefficient between sequencing lineage cells according to gene expression, and used Ward's method (ward.D) for hierarchical clustering. For better understanding of the relationship among mouse BTSCs, mouse AHeps, human AHeps, human BTSCs, human HpSCs, human HBs and human AHeps, correlation analyses were performed and correlation heatmap was plotted for visualization.

5.14. Principal component analysis

Principal component analysis (PCA) can show the relationship between samples/maturational lineage staged cells from different dimensions. The closer the sample clustering distance or PCA distance is, the more similar the samples/lineage-staged cells are. The samples/lineage-staged cells of each group are distributed in different areas of two-dimensional or three-dimensional space, and the samples of the same group are more concentrated in the spatial distribution. Using the PCA pipeline, we compared the transcriptomic characteristics of mouse maturational lineage-staged cells with that of human maturational lineage-staged cells to better confirming the successful isolation and culture of mouse BTSCs.

5.15. Differential expression analysis and enrichment analysis

We used the DESeq2 software in R to standardize the number of gene counts of each sample (using the BaseMean value to estimate the expression level) and screen differential protein-coding genes based on the multiple of difference and the results of the significant difference test. After the differentially expressed genes were obtained, the KEGG database was leveraged to conduct enrichment analysis on DEGs and the hypergeometric distribution test method was used to calculate the significance of differential gene enrichment in each Pathway entry. We selected the top 20 enriched terms of KEGG enrichment analysis (filtering the Pathway entries corresponding to p-value) to draw bubble diagrams.

5.16. Stem-cell-patch grafting

In past studies, engraftment was found to require co-transplantation of epithelial cells with their maturational lineage-stage-appropriate mesenchymal cell partners. The mesenchymal cells needed for biliary tree stem cells (BTSCs) were comprised of angioblasts ($CD117^+$, $CD133^+$, $VEGFr^+$, CD31-negative) and their immediate descendants, precursors to endothelia ($CD133^+$, $VEGFr^+$, $CD31^+$, Von Willebrand $Factor^+$) and precursors to stellate cells [$CD146^+$, $ICAM\text{-}1^+$, alpha-smooth muscle $actin^+$ (ASMA), vitamin A-negative]. We refer to these collectively as early lineage-stage-mesenchymal-cells (ELSMCs). The organoids are floating aggregates of BTSCs and ELSMCs and referred to as BTSC/ELSMCs. In the BEX-gel system, the $EpCAM^+$ cells were 85 % of the total cells that were obtained from each passage, leaving the rest (~15 %) as ELSMCs. Once we obtained stable expanded BTSC/ELSMCs either in 2D monolayer cultures or the organoids in the 3D BEX-system, they were collected and prepared as patch grafts using methods established previously to enable the direct engraftment of BTSC organoids into the $Fah^{-/-}$ liver injury animals.

Stem-Cell-Patch Graft Composition. Grafts were secured to the organ surface by sutures or surgical glue (at the edges of the graft) as shown in Fig. 8. The graft composition involved the use of thiol-modified hyaluronans (HA) hydrogels prepared with precise concentrations of HA and PEGDA to achieve defined levels of stiffness, as determined rheologically and expressed as the dynamic shear modulus (G*). Donor cells were embedded into a soft HA layer (viscoelasticity of less than 100 Pa) and placed against the organ surface, covered with the backing of GelFoam that was then glued to the target site at the corners with surgical glue. It was coated then with a version of the thiol-hyaluronan triggered to make a hydrogel of ~200–300 Pa to prevent any adhesive or abrasive adverse events related to the grafting. Engraftment of the donor organoids occurs within hours and is completed within the target organ within a week. Once engrafted, the biomaterials of the graft, such as the hyaluronans and the GelFoam backing are cleared or eliminated by the host organ, leaving the native soluble signals and matrix components of the organ to dictate maturation of the donor cells to an adult fate.

5.17. Quantification and statistical analysis

Statistically significant differences between samples were calculated by using Student's 2-tailed *t*-test or One-way ANOVA, and results are presented as the mean ± standard deviation (SD). One-way ANOVA was used in the case of multiple group comparisons, including Fig. 4D, S2C and 7C. The *t*-test was used in the other data (Figs. 1F, 2D and 2F, 3D, 3F, 4C, 4E, 5B-C, 5G, 5I, 6B–C, 6E-F, 8E, 8I, S1C, S2D-E S6A-C). Especially, Figs. 2F, 3D and 3F, 4E, 5B-C, 8I and S6C show the results of ≥3 groups, but with the purpose of comparing the difference between different cell types or the difference between experimental group and specific control group, *t*-test was applied to compare the results of specific two groups in the case. The p-values less than 0.05, 0.01 and 0.001 were considered statistically significant, shown as "a", "b", and "c", respectively.

CRediT authorship contribution statement

Wencheng Zhang: Writing – review & editing, Writing – original draft, Visualization, Validation, Supervision, Resources, Project

administration, Methodology, Investigation, Funding acquisition, Formal analysis, Conceptualization. **Yangyang Cui:** Writing – review & editing, Writing – original draft, Methodology, Investigation, Data curation. **Mengqi Lu:** Writing – review & editing, Writing – original draft, Validation, Methodology, Formal analysis, Data curation. **Mingyang Xu:** Validation, Methodology. **Yuting Li:** Validation, Data curation. **Haimeng Song:** Validation, Methodology. **Yi Luo:** Validation, Data curation. **Jinjia Song:** Validation, Data curation. **Yong Yang:** Methodology, Data curation. **Xicheng Wang:** Validation, Data curation. **Lijun Liao:** Validation, Resources, Funding acquisition. **Yunfang Wang:** Resources, Methodology, Funding acquisition. **Lola Reid:** Writing – review & editing, Writing – original draft, Validation, Supervision, Investigation, Funding acquisition, Formal analysis. **Zhiying He:** Writing – review & editing, Validation, Supervision, Software, Resources, Methodology, Funding acquisition, Formal analysis.

Declaration of competing interest

All authors declare that there are no competing interests.

Acknowledgements

This work was funded by the Major Program of National Key Research and Development Project (2020YFA0112600, 2019YFA0801502), the National Natural Science Foundation of China (82173019, 82270638, 8220374, 82300718), the Project of Shanghai Science and Technology Commission (22ZR1451100, 22Y11908500), the Peak Disciplines (Type IV) of Institutions of Higher Learning in Shanghai, and Shanghai Engineering Research Center of Stem Cells Translational Medicine (20DZ2255100).

LMR and her associates and their studies were funded by the UNC School of Medicine, the Fibrolamellar Carcinoma Foundation (Greenwich, CT) and by multiple NIH Core and Center grants (5P41EB002025); Center for Gastrointestinal and Biliary Disease Biology (NIDDK Grant: P30 DK034987); and the Lineberger Cancer Center grant (NCI grant # CA016086).LJL was funded by Shanghai 2023 “Technology Innovation Action Plan” medical innovation research project (23Y11908300), the Academic Medical Leaders Training Program in Health System of Pudong New Area (PWRd2020-06), Shanghai Pudong New Area summit (emergency medicine and critical care) construction project (PWYgf2021-03), and National Natural Science Foundation of China (82202401, 82170089).YFW was funded by the National Key Research and Development Program of China (2022YFA1103400) and National Natural Science Foundation of China (92168207).The authors kindly thank Professor Jian Liu at the Division of Chemical Biology and Medicinal Chemistry, Eshelman School of Pharmacology, University of North Carolina (Chapel Hill, NC) for providing suggestions for revisions. We thank Dr. Weixia Kong (Graduate School of Frontier Biosciences, Osaka University, Suita, Osaka, 565–0871, Japan) for her support on preparing the schematic graph.

Appendix A. Supplementary data

Supplementary data to this article can be found online at https://doi.org/10.1016/j.bioactmat.2024.08.010.

References

[1] G. Carpino, V. Cardinale, P. Onori, A. Franchitto, P.B. Berloco, M. Rossi, Y. Wang, R. Semeraro, M. Anceschi, R. Brunelli, D. Alvaro, L.M. Reid, E. Gaudio, Biliary tree stem/progenitor cells in glands of extrahepatic and intrahepatic bile ducts: an anatomical in situ study yielding evidence of maturational lineages, J. Anat. 220 (2) (2012) 186–199, https://doi.org/10.1111/j.1469-7580.2011.01462.x.

[2] Y. Wang, G. Lanzoni, G. Carpino, C. Cui, J. Dominguez-Bendala, E. Wauthier, V. Cardinale, T. Oikawa, A. Pilegg, D. Gerber, M.E. Furth, D. Alvaro, E. Gaudio, L. Inverardi, L.M. Reid, Biliary tree stem cells, precursors to pancreatic committed progenitors: evidence for life-long pancreatic organogenesis *Stem cells* 31 (9) (2013) 1966–1979.

[3] W. Zhang, G. Lanzoni, H. Hani, D. Overi, V. Cardinale, S. Simpson, W. Pitman, A. Allen, X. Yi, X. Wang, D. Gerber, G. Prestwich, O. Lozoya, E. Gaudio, D. Alvaro, D. Tokaz, J. Dominguez-Bendala, C. Adin, J. Piedrahita, L.M. Reid, Patch grafting, strategies for transplantation of organoids into solid organs such as liver, Biomaterials 277 (2021) 121067, https://doi.org/10.1016/j.biomaterials.2021.121067.

[4] W. Zhang, X. Wang, G. Lanzoni, E. Wauthier, S. Simpson, J.A. Ezzell, A. Allen, C. Suitt, J. Krolik, A. Jhirad, J. Dominguez-Bendala, V. Cardinale, D. Alvaro, D. Overi, E. Gaudio, P. Sethupathy, G. Carpino, C. Adin, J.A. Piedrahita, L.M. Reid, A postnatal network of co-hepato/pancreatic stem/progenitors in the biliary trees of pigs and humans, NPJ Regen Med 8 (1) (2023) 40, https://doi.org/10.1038/s41536-023-00303-5.

[5] W. Zhang, E. Wauthier, G. Lanzoni, H. Hani, X. Yi, D. Overi, L. Shi, S. Simpson, A. Allen, C. Suitt, J.A. Ezzell, D. Alvaro, V. Cardinale, E. Gaudio, G. Carpino, G. Prestwich, J. Dominguez-Bendala, D. Gerber, K. Mathews, L.M. Reid, Patch grafting of organoids of stem/progenitors into solid organs can correct genetic-based disease states, Biomaterials 288 (2022) 121647, https://doi.org/10.1016/j.biomaterials.2022.121647.

[6] V. Cardinale, G. Carpino, R. Gentile, C. Napoletano, H. Rahimi, A. Franchitto, R. Semeraro, M. Nuti, P. Onori, P.B. Berloco, M. Rossi, D. Bosco, R. Brunelli, A. Fraveto, C. Napoli, A. Torrice, M. Gatto, R. Venere, C. Bastianelli, D. Alvaro, Transplantation of human fetal biliary tree stem/progenitor cells into two patients with advanced liver cirrhosis, BMC Gastroenterol. 14 (2014) 204, https://doi.org/10.1186/s12876-014-0204-z.

[7] A.A. Khan, N. Parveen, V.S. Mahaboob, A. Rajendraprasad, H.R. Ravindraprakash, J. Venkateswarlu, P. Rao, G. Pande, M.L. Narusu, M.N. Khaja, R. Pramila, A. Habeeb, C.M. Habibullah, Management of hyperbilirubinemia in biliary atresia by hepatic progenitor cell transplantation through hepatic artery: a case report, Transplant. Proc. 40 (4) (2008) 1153–1155, https://doi.org/10.1016/j.transproceed.2008.03.110.

[8] A.A. Khan, N. Parveen, V.S. Mahaboob, A. Rajendraprasad, H.R. Ravindraprakash, J. Venkateswarlu, P. Rao, G. Pande, M.L. Narusu, M.N. Khaja, R. Pramila, A. Habeeb, C.M. Habibullah, Treatment of Crigler-Najjar Syndrome type 1 by hepatic progenitor cell transplantation: a simple procedure for management of hyperbilirubinemia, Transplant. Proc. 40 (4) (2008) 1148–1150, https://doi.org/10.1016/j.transproceed.2008.03.022.

[9] A.A. Khan, M.V. Shaik, N. Parveen, A. Rajendraprasad, M.A. Aleem, M.A. Habeeb, G. Srinivas, T.A. Raj, S.K. Tiwari, K. Kumaresan, J. Venkateswarlu, G. Pande, C. M. Habibullah, Human fetal liver-derived stem cell transplantation as supportive modality in the management of end-stage decompensated liver cirrhosis, Cell Transplant. 19 (4) (2010) 409–418, https://doi.org/10.3727/096368910X498241.

[10] H. Kubota, L.M. Reid, Clonogenic hepatoblasts, common precursors for hepatocytic and biliary lineages, are lacking classical major histocompatibility complex class I antigens, Proceedings of the National Academy of Sciences of the USA 97 (22) (2000) 12132–12137.

[11] H. Kubota, H.-l. Yao, L.M. Reid, Identification and characterization of vitamin A-storing cells in fetal liver: implications for functional importance of hepatic stellate cells in liver development and hematopoiesis, Stem Cells (Dayton) 25 (9) (2007) 2339–2349. doi:10.1634/stemcells.2006-0316.

[12] O.A. Lozoya, W. E, R. Turner, C. Barbier, G.D. Prestwich, F. Guilak, R. Superfine, S. R. Lubkin, L.M. Reid, Regulation of hepatic stem/progenitor phenotype by microenviroment stiffness in hydrogel models of the human liver stem cell niche, Biomaterials 32 (30) (2011) 7389–7402, https://doi.org/10.1016/j.biomaterials.2011.06.042.

[13] H. Kubota, M.R. Avarbock, R.L. Brinster, Culture conditions and single growth factors affect fate determination of mouse spermatogonial stem cells, Biol. Reprod. 71 (3) (2004) 722–731. doi: 10.1095/biolreprod.104.029207.

[14] R. Turner, E. Wauthier, O. Lozoya, R. McClelland, J. Bowsher, C. Barbier, D. Gerber, G. Prestwich, E. Hsu, L.M. Reid, Successful transplantation of human hepatic stem cells with restricted localization to liver using hyaluronan grafts, Hepatology 57 (2013) 775–784.

[15] Y. Wang, H. Yao, C. Barbier, E. Wauthier, C. Cui, N. Moss, M. Yamauchi, M. Sricholpech, M.J. Costello, D. Gerber, E.G. Loboa, L.M. Reid, Lineage-dependent epithelial-mesenchymal paracrine signals dictate growth versus differentiation of human hepatic stem cells to adult fates, Hepatology 52 (4) (2010) 1443–1454.

[16] G. Benton, I. Arnaoutova, J. George, H.K. Kleinman, J. Koblinski, Matrigel: from discovery and ECM mimicry to assays and models for cancer research, Adv. Drug Deliv. Rev. 79–80 (2014) 3–18, https://doi.org/10.1016/j.addr.2014.06.005.

[17] C.S. Hughes, L.M. Postovit, G.A. Lajoie, Matrigel: a complex protein mixture required for optimal growth of cell culture, Proteomics 10 (9) (2010) 1886–1890, https://doi.org/10.1002/pmic.200900758.

[18] H.K. Kleinman, M.L. McGarvey, L.A. Liotta, P.G. Robey, K. Tryggvason, G. R. Martin, Isolation and characterization of type IV procollagen, laminin, and heparan sulfate proteoglycan from the EHS sarcoma, Biochemistry 21 (24) (1982) 6188–6193, https://doi.org/10.1021/bi00267a025.

[19] L.K. Robinson, V.A. Murrah, M.P. Moyer, D.H. Rohrbach, Characterization of a novel glycoprotein isolated from the basement membrane matrix of the Engelbreth-Holm-Swarm tumor, J. Biol. Chem. 264 (9) (1989) 5141–5147.

[20] S. Vukicevic, F.P. Luyten, H.K. Kleinman, A.H. Reddi, Differentiation of canalicular cell processes in bone cells by basement membrane matrix components: regulation by discrete domains of laminin, Cell 63 (2) (1990) 437–445. https://pubmed.ncbi.nlm.nih.gov/2208292.

[21] E.A. Aisenbrey, W.L. Murphy, Synthetic alternatives to matrigel, Nat. Rev. Mater. 5 (7) (2020) 539–551, https://doi.org/10.1038/s41578-020-0199-8.

[22] F. Kaluthantrige Don, M. Huch, Organoids, where we stand and where we go, Trends Mol. Med. 27 (5) (2021) 416–418, https://doi.org/10.1016/j.molmed.2021.03.001.
[23] S. Kaur, I. Kaur, P. Rawal, D.M. Tripathi, A. Vasudevan, Non-matrigel scaffolds for organoid cultures, Cancer Lett. 504 (2021) 58–66, https://doi.org/10.1016/j.canlet.2021.01.025.
[24] M.T. Kozlowski, C.J. Crook, H.T. Ku, Towards organoid culture without Matrigel, Commun. Biol. 4 (1) (2021) 1387, https://doi.org/10.1038/s42003-021-02910-8.
[25] A. Marchini, F. Gelain, Synthetic scaffolds for 3D cell cultures and organoids: applications in regenerative medicine, Crit. Rev. Biotechnol. 42 (3) (2022) 468–486, https://doi.org/10.1080/07388551.2021.1932716.
[26] A.B. Francisco, J. Li, A.R. Farghli, M. Kanke, B. Shui, P.R. Munn, J.K. Grenier, P. D. Soloway, Z. Wang, L.M. Reid, J. Liu, P. Sethupathy, Chemical, molecular, and single-nucleus analysis reveal chondroitin sulfate proteoglycan aberrancy in fibrolamellar carcinoma, Cancer Res Commun 2 (7) (2022) 663–678, https://doi.org/10.1158/2767-9764.Crc-21-0177.
[27] W.S. Turner, E. Schmelzer, R. McClelland, E. Wauthier, W. Chen, L.M. Reid, Human hepatoblast phenotype maintained by hyaluronan hydrogels, J. Biomed. Mater. Res., Part B 82 (1) (2007) 156–168. doi: 10.1002/jbm.b.30717.
[28] G. Carpino, A. Renzi, A. Franchitto, V. Cardinale, P. Onori, L. Reid, D. Alvaro, E. Gaudio, Stem/progenitor cell niches involved in hepatic and biliary regeneration, Stem Cell. Int. 2016 (2016) 3658013, https://doi.org/10.1155/2016/3658013.
[29] V. Cardinale, Y. Wang, G. Carpino, C.B. Cui, M. Gatto, M. Rossi, P. Bartolomeo Berloco, A. Cantafora, E. Wauthier, M.E. Furth, Multipotent stem/progenitor cells in human biliary tree give rise to hepatocytes, cholangiocytes, and pancreatic islets, Hepatology 54 (6) (2011) 2159–2172, https://doi.org/10.1002/hep.24590.
[30] G. Carpino, V. Cardinale, R. Gentile, P. Onori, R. Semeraro, A. Franchitto, Y. Wang, D. Bosco, A. Iossa, C. Napoletano, A. Cantafora, G. D'Argenio, M. Nuti, N. Caporaso, P. Berloco, R. Venere, T. Oikawa, L. Reid, D. Alvaro, E. Gaudio, Evidence for multipotent endodermal stem/progenitor cell populations in human gallbladder, J. Hepatol. 60 (6) (2014) 1194–1202, https://doi.org/10.1016/j.jhep.2014.01.026.
[31] W. Zhang, Y. Xu, X. Wang, T. Oikawa, G. Su, E. Wauthier, G. Wu, P. Sethupathy, Z. He, J. Liu, L.M. Reid, Fibrolamellar carcinomas-growth arrested by paracrine signals complexed with synthesized 3-O sulfated heparan sulfate oligosaccharides, Matrix Biol.: Journal of the International Society For Matrix Biology 121 (2023) 194–216, https://doi.org/10.1016/j.matbio.2023.06.008.
[32] X. Wang, W. Zhang, Y. Yang, J. Wang, H. Qiu, L. Liao, T. Oikawa, E. Wauthier, P. Sethupathy, L.M. Reid, Z. Liu, Z. He, A MicroRNA-based network provides potential predictive signatures and reveals the crucial role of PI3K/AKT signaling for hepatic lineage maturation, Front. Cell Dev. Biol. 9 (2021), https://doi.org/10.3389/fcell.2021.670059.
[33] G. Carpino, A. Renzi, V. Cardinale, A. Franchitto, P. Onori, D. Overi, M. Rossi, P. B. Berloco, D. Alvaro, L.M. Reid, E. Gaudio, Progenitor cell niches in the human pancreatic duct system and associated pancreatic duct glands: an anatomical and immunophenotyping study, J. Anat. 228 (3) (2016) 474–486, https://doi.org/10.1111/joa.12418.
[34] V. Cardinale, G. Carpino, D. Overi, S. Safarikia, W. Zhang, M. Kanke, A. Franchitto, D. Costantini, O. Riccioni, L. Nevi, M. Chiappetta, P. Onori, M. Franchitto, S. Bini, Y.H. Hung, Q. Lai, I. Zizzari, M. Nuti, C. Nicoletti, E. Gaudio, Human duodenal submucosal glands contain a defined stem/progenitor subpopulation with liver-specific regenerative potential, J. Hepatol. 78 (1) (2023) 165–179, https://doi.org/10.1016/j.jhep.2022.08.037.
[35] Y. Wang, J. Qin, S. Wang, W. Zhang, J. Duan, J. Zhang, X. Wang, F. Yan, M. Chang, X. Liu, B. Feng, J. Liu, X. Pei, Conversion of human gastric epithelial cells to multipotent endodermal progenitors using defined small molecules, Cell Stem Cell 19 (4) (2016) 449–461, https://doi.org/10.1016/j.stem.2016.06.006.
[36] F. Yan, Y. Wang, W. Zhang, M. Chang, Z. He, J. Xu, C. Shang, T. Chen, J. Liu, X.J. H. Wang, Human embryonic stem cell–derived hepatoblasts are an optimal lineage stage for hepatitis C virus infection, Hepatology 66 (3) (2017) 717–735, https://doi.org/10.1002/hep.29134.
[37] W. Zhang, A. Allen, E. Wauthier, X. Yi, H. Hani, P. Sethupathy, D. Gerber, V. Cardinale, G. Carpino, J. Dominguez-Bendala, Stem cell-fueled maturational lineages in hepatic and pancreatic organogenesis, Liver: Biology and Pathobiology (2020) 521–538.
[38] J.D. Esko, U. Lindahl, Molecular diversity of heparan sulfate, J. Clin. Invest. 108 (2001) 169–173.
[39] J. Yang, P.H. Hsieh, X. Liu, W. Zhou, X. Zhang, J. Zhao, J. Xu, F. Zhang, R. J. Linhardt, J. Liu, Construction and characterization of heparan sulfate heptasaccharide microarray, Chem. Commun. 53 (2017) 1743–1746.
[40] B.I. Ayerst, C.L.R. Merry, A.J. Day, The good the bad and the ugly of glycosaminoglycans in tissue engineering applications, Pharmaceuticals 10 (2) (2017) 54, https://doi.org/10.3390/ph10020054.
[41] J.R. Couchman, H. Multhaupt, R.D. Sanderson, Recent Insights into Cell Surface Heparan Sulphate Proteoglycans and Cancer (Review, eCollection), 2016, https://doi.org/10.12688/f1000research.8543.1. F1000 Faculty Rev. , pii: F1000 Faculty Rev-1541.
[42] J.D. Esko, S.B. Selleck, Order out of chaos: assembly of ligand binding sites in heparan sulfate, Annu. Rev. Biochem. 71 (2002) 435–471.
[43] W.C. Lamanna, I. Kalus, M. Padva, R.J. Baldwin, C.L. Merry, T. Dierks, The heparanome–the enigma of encoding and decoding heparan sulfate sulfation, J. Biotechnol. 129 (2) (2007) 290–307, https://doi.org/10.1016/j.jbiotec.2007.01.022.
[44] V.N. Patel, D.L. Pineda, M.P. Hoffman, The function of heparan sulfate during branching morphogenesis, Matrix Biol. : Journal of the International Society For Matrix Biology 57–58 (2017) 311–323, https://doi.org/10.1016/j.matbio.2016.09.004.
[45] A. Theodoraki, Y. Hu, S. Poopalasundaram, A. Oosterhof, S.E. Guimond, P. Disterer, B. Khoo, A.C. Hauge-Evans, P.M. Jones, J.E. Turnbull, T.H. van Kuppevelt, P.-M. Bouloux, Distinct patterns of heparan sulphate in pancreatic islets suggest novel roles in paracrine islet regulation, Mol. Cell. Endocrinol. 399 (2015) 296–310, https://doi.org/10.1016/j.mce.2014.09.011.
[46] D. Xu, K. Arnold, J. Liu, Using structurally defined oligosaccharides to understand the interactions between proteins and heparan sulfate, Curr. Opin. Struct. Biol. 50 (2018) 155–161, https://doi.org/10.1016/j.sbi.2018.04.003.
[47] J.L. Vanderhooft, M. Alcoutlabi, J.J. Magda, G.D. Prestwich, Rheological properties of cross-linked hyaluronan-gelatin hydrogels for tissue engineering, Macromol. Biosci. 9 (1) (2009) 20–28. doi:10.1002/mabi.200800141.
[48] Y. Bai, Z. Yang, X. Xu, W. Ding, J. Qi, F. Liu, X. Wang, B. Zhou, W. Zhang, X. Zhuang, G. Li, Y. Zhao, Direct chemical induction of hepatocyte-like cells with capacity for liver repopulation, Hepatology 77 (5) (2023) 1550–1565, https://doi.org/10.1002/hep.32686.
[49] K. Li, S. Zhu, H.A. Russ, S. Xu, T. Xu, Y. Zhang, T. Ma, M. Hebrok, S. Ding, Small molecules facilitate the reprogramming of mouse fibroblasts into pancreatic lineages, Cell Stem Cell 14 (2) (2014) 228–236, https://doi.org/10.1016/j.stem.2014.01.006.
[50] W. Li, S. Ding, Small molecules that modulate embryonic stem cell fate and somatic cell reprogramming, Trends Pharmacol. Sci. 31 (1) (2010) 36–45, https://doi.org/10.1016/j.tips.2009.10.002.
[51] H. Wang, N. Cao, C.I. Spencer, B. Nie, T. Ma, T. Xu, Y. Zhang, X. Wang, D. Srivastava, S. Ding, Small molecules enable cardiac reprogramming of mouse fibroblasts with a single factor, Oct4, Cell Rep. 6 (5) (2014) 951–960, https://doi.org/10.1016/j.celrep.2014.01.038.
[52] Y. Rautureau, M. Berlatie, D. Rivas, K. Uy, A. Blanchette, G. Miquel, M. Higgins, M. Mecteau, A. Nault, L. Villeneuve, V. Lavoie, G. Théberge-Julien, G. Brand, L. Lapointe, M. Denis, C. Rosa, A. Fortier, L. Blondeau, M.C. Guertin, J.C. Tardif, Adenylate cyclase type 9 antagonizes cAMP accumulation and regulates endothelial signalling involved in atheroprotection, Cardiovasc. Res. 119 (2) (2023) 450–464, https://doi.org/10.1093/cvr/cvac085.
[53] G. Wang, D. Zhang, L. Qin, Q. Liu, W. Tang, M. Liu, F. Xu, F. Tang, L. Cheng, H. Mo, X. Yuan, Z. Wang, B. Huang, Forskolin-driven conversion of human somatic cells into induced neurons through regulation of the cAMP-CREB1-JNK signaling, Theranostics 14 (4) (2024) 1701–1719, https://doi.org/10.7150/thno.92700.
[54] M.A. Bochenek, O. Veiseh, A.J. Vegas, J.J. McGarrigle, M. Qi, E. Marchese, M. Omami, J.C. Doloff, J. Mendoza-Elias, M. Nourmohammadzadeh, A. Khan, C.-C. Yeh, Y. Xing, D. Isa, S. Ghani, J. Li, C. Landry, A.R. Bader, K. Olejnik, J. Oberholzer, Alginate encapsulation as long-term immune protection of allogeneic pancreatic islet cells transplanted into the omental bursa of macaques, Nat. Biomed. Eng. 2 (11) (2018) 810–821, https://doi.org/10.1038/s41551-018-0275-1.
[55] B.A. Nerger, S. Sinha, N.N. Lee, M. Cheriyan, P. Bertsch, C.P. Johnson, L. Mahadevan, J.V. Bonventre, D.J. Mooney, 3D hydrogel encapsulation regulates nephrogenesis in kidney organoids, Adv. Mater. 36 (14) (2024) e2308325, https://doi.org/10.1002/adma.202308325.
[56] X. Yuan, J. Wu, Z. Sun, J. Cen, Y. Shu, C. Wang, H. Li, D. Lin, K. Zhang, B. Wu, A. Dhawan, L. Zhang, L. Hui, Preclinical efficacy and safety of encapsulated proliferating human hepatocyte organoids in treating liver failure, Cell Stem Cell 31 (4) (2024) 484–498.e485, https://doi.org/10.1016/j.stem.2024.02.005.
[57] T. Gao, X. Zhao, J. Hao, Y. Tian, H. Ma, W. Liu, B. An, F. Sun, S. Liu, B. Guo, S. Niu, Z. Li, C. Wang, Y. Wang, G. Feng, L. Wang, W. Li, J. Wu, M. Guo, Q. Gu, A scalable culture system incorporating microcarrier for specialised mesenchymal stem cells from human embryonic stem cells, Materials Today. Bio 20 (2023) 100662, https://doi.org/10.1016/j.mtbio.2023.100662.
[58] H.J. Kim, J.M. Park, S. Lee, S.J. Hong, J.I. Park, M.S. Lee, H.S. Yang, J.S. Park, K. H. Park, In situ pocket-type microcarrier (PMc) as a therapeutic composite: regeneration of cartilage with stem cells, genes, and drugs, J. Contr. Release 332 (2021) 337–345, https://doi.org/10.1016/j.jconrel.2020.08.057.
[59] Z. Gao, J. Guo, B. Gou, Z. Gu, T. Jia, S. Ma, L. Jiang, W. Liu, L. Zhou, Q. Gu, Microcarriers promote the through interface movement of mouse trophoblast stem cells by regulating stiffness, Bioact. Mater. 28 (2023) 196–205, https://doi.org/10.1016/j.bioactmat.2023.05.007.
[60] M. Grieco, O. Ursini, I.E. Palamà, G. Gigli, L. Moroni, B. Cortese, HYDRHA: hydrogels of hyaluronic acid. New biomedical approaches in cancer, neurodegenerative diseases, and tissue engineering, Materials Today. Bio 17 (2022) 100453, https://doi.org/10.1016/j.mtbio.2022.100453.
[61] G.D. Prestwich, D.M. Marecak, J.F. Marecak, K.P. Vercruysse, M.R. Ziebell, Controlled chemical modification of hyaluronic acid: synthesis, applications, and biodegradation of hydrazide derivatives, J. Contr. Release 53 (1998) 93–103.
[62] K.R. Kirker, G.D. Prestwich, Physical properties of glycosaminoglycan hydrogels, J. Polym. Sci. B Polym. Phys. 42 (2004) 4344–4356.
[63] Y. Luo, K.R. Kirker, G.D. Prestwich, Cross-linked hyaluronic acid hydrogel films: New biomaterials for drug delivery, J. Contr. Release 69 (2000) 169–184.
[64] T. Pouyani, G.S. Harbison, G.D. Prestwich, Novel hydrogels of hyaluronic acid: synthesis, surface morphology, and solid-state NMR, J. Am. Chem. Soc. 116 (1994) 7515–7522.
[65] X.Z. Shu, S. Ahmad, Y. Liu, G.D. Prestwich, Synthesis and evaluation of injectable, in situ crosslinkable synthetic extracellular matrices for tissue engineering, J. Biomed. Mater. Res. 29 (2006) 29.
[66] E. Kostallari, B. Wei, D. Sicard, J. Li, S.A. Cooper, J. Gao, M. Dehankar, Y. Li, S. Cao, M. Yin, D.J. Tschumperlin, V.H. Shah, Stiffness is associated with hepatic

stellate cell heterogeneity during liver fibrosis, Am. J. Physiol. Gastrointest. Liver Physiol. 322 (2) (2022) G234–G246, https://doi.org/10.1152/ajpgi.00254.2021.
[67] A. Abalymov, L. Van der Meeren, M. Saveleva, E. Prikhozhdenko, K. Dewettinck, B. Parakhonskiy, A.G. Skirtach, Cells-Grab-on particles: a novel approach to control cell focal adhesion on hybrid thermally annealed hydrogels, ACS Biomater. Sci. Eng. 6 (7) (2020) 3933–3944, https://doi.org/10.1021/acsbiomaterials.0c00119.
[68] J.A. Marcum, D.H. Atha, L.M. Fritze, P. Nawroth, D. Stern, R.D. Rosenberg, Cloned bovine aortic endothelial cells synthesize anticoagulantly active heparan sulfate proteoglycan, J. Biol. Chem. 261 (16) (1986) 7507–7517. https://pubmed.ncbi.nlm.nih.gov/2940242.
[69] G. Pejler, G. Bäckström, U. Lindahl, M. Paulsson, M. Dziadek, S. Fujiwara, R. Timpl, Structure and affinity for antithrombin of heparan sulfate chains derived from basement membrane proteoglycans, J. Biol. Chem. 262 (11) (1987) 5036–5043. https://pubmed.ncbi.nlm.nih.gov/2951375.
[70] B.E. Thacker, D. Xu, R. Lawrence, J.D. Esko, Heparan sulfate 3-O-sulfation: a rare modification in search of a function, Matrix Biol. : Journal of the International Society For Matrix Biology 35 (2014) 60–72, https://doi.org/10.1016/j.matbio.2013.12.001.
[71] Z. Wang, K. Arnold, V.M. Dhurandahare, Y. Xu, V. Pagadala, E. Labra, W. Jeske, J. Fareed, M. Gearing, J. Liu, Analysis of 3-O-sulfated heparan sulfate using isotopically labeled oligosaccharide calibrants, Anal. Chem. 94 (6) (2022) 2950–2957, https://doi.org/10.1021/acs.analchem.1c04965.
[72] Z. Wang, K. Arnold, V.M. Dhurandhare, Y. Xu, J. Liu, Investigation of the biological functions of heparan sulfate using a chemoenzymatic synthetic approach, RSC Chemical Biology 2 (3) (2021) 702–712, https://doi.org/10.1039/d0cb00199f.
[73] V.N. Patel, I.M.A. Lolbaert, S.N. Cowherd, N.W. Shworak, Y. Xu, J. Liu, M. P. Hoffman, Hs3st3-modified heparan sulfate controls KIT+ progenitor expansion by regulating 3-O-sulfotransferases, Dev Cell. 29 (6) (2014) 662–673, https://doi.org/10.1016/j.devcel.2014.04.024.
[74] G. Lanzoni, T. Oikawa, Y. Wang, C.B. Cui, G. Carpino, V. Cardinale, D. Gerber, M. Gabriel, J. Dominguez-Bendala, M.E. J.S.c. Furth, Concise review: clinical programs of stem cell therapies for liver and pancreas, Stem Cell. 31 (10) (2013) 2047–2060, https://doi.org/10.1002/stem.1457.
[75] E. Wauthier, R. McClelland, W. Turner, E. Schmelzer, H. Kubota, L. Zhang, J. Ludlow, A. Bruce, H. Yao, M.E. Furth, E. LeCluyse, N. Moss, R. Turner, P. Merrick, C. Barbier, O. Lozoya, J. Ruiz, L.M. Reid, Hepatic stem cells and hepatoblasts: identification, isolation and *ex vivo* maintenance *Methods for Cell Biology (Methods for Stem Cells)* 86 (2008) 137–225.